Journal of Cardiothoracic and Vascular Anesthesia 33 (2019) 1559–1583

Contents lists available at ScienceDirect

Journal of Cardiothoracic and Vascular Anesthesia

journal homepage: www.jcvaonline.com

Expert Review

Echocardiographic Applications of M-Mode Ultrasonography in Anesthesiology and Critical Care

Gabriel Prada, MD[*], Antoine Vieillard-Baron, MD[†,‡,§], Archer K. Martin, MD[¶], Antonio Hernandez, MD[‖], Farouk Mookadam, MD[#], Harish Ramakrishna, MD[**,1], Jose L. Diaz-Gomez, MD[*,¶,††]

[*]*Department of Critical Care Medicine, Mayo Clinic, Jacksonville, FL*
[†]*Intensive Care Unit, Assistance Publique-Hôpitaux de Paris, University Hospital Ambroise Paré, Boulogne-Billancourt, France*
[‡]*Faculty of Medicine Paris Ile-de-France Ouest, University of Versailles Saint-Quentin en Yvelines, Saint-Quentin En Yvelines, France*
[§]*INSERM U-1018, CESP, Team 5, University of Versailles Saint-Quentin en Yvelines, Villejuif, France*
[¶]*Department of Anesthesiology and Perioperative Medicine, Mayo Clinic, Jacksonville, FL*
[‖]*Department of Anesthesiology, Vanderbilt University Medical Center, Nashville, TN*
[#]*Department of Cardiovascular Diseases, Mayo Clinic, Scottsdale, AZ*
[**]*Department of Anesthesiology and Perioperative Medicine, Mayo Clinic Hospital, Phoenix, AZ*
[††]*Department of Neurologic Surgery, Mayo Clinic, Jacksonville, FL*

Proficiency in echocardiography and lung ultrasound has become essential for anesthesiologists and critical care physicians. Nonetheless, comprehensive echocardiography measurements often are time-consuming and technically challenging, and conventional 2-dimensional images do not permit evaluation of specific conditions (eg, systolic anterior motion of the mitral valve, pneumothorax), which have important clinical implications in the perioperative setting. M-mode (motion-based) ultrasonographic imaging, however, provides the most reliable temporal resolution in ultrasonography. Hence, M-mode can provide clinically relevant information in echocardiography and lung ultrasound–driven approaches for diagnosis, monitoring, and interventional procedures performed by anesthesiologists and intensivists. Although M-mode is feasible, this imaging modality progressively has been abandoned in echocardiography and is often underutilized in lung ultrasound. This article aims to comprehensively illustrate contemporary applications of M-mode ultrasonography in the anesthesia and critical care medicine practice. Information presented for each clinical application will include image acquisition and interpretation, evidence-based clinical implications in the critically ill and surgical patient, and limitations. The present article focuses on echocardiography and reviews left ventricular function (mitral annular plane systolic excursion, E-point septal separation, fractional shortening, and transmitral propagation velocity); right ventricular function (tricuspid annular plane systolic excursion, subcostal echocardiographic assessment of tricuspid annulus kick, outflow tract fractional shortening, ventricular septal motion, wall thickness, and outflow tract obstruction); volume status and responsiveness (inferior vena cava and superior vena cava diameter and respiratory variability [collapsibility and distensibility indexes]); cardiac tamponade; systolic anterior motion of the mitral valve; and aortic dissection.

Key Words: anesthesia; critical care; echocardiography; lung ultrasound; M-mode; ultrasonography

ULTRASONOGRAPHY WAS FIRST introduced into clinical practice as echocardiography.[1] More than half a century after the first report, ultrasonography is used in almost all medical specialties,[2] and echocardiography and lung ultrasound

[1]*Address reprint requests to* Harish Ramakrishna, MD, Department of Anesthesiology and Perioperative Medicine, Mayo Clinic Hospital, 5777 East Mayo Blvd., Phoenix, AZ 85054.
E-mail address: Ramakrishna.harish@mayo.edu (H. Ramakrishna).

https://doi.org/10.1053/j.jvca.2018.06.019
1053-0770/

(LUS) are being increasingly used in anesthesiology and critical care. This advance is due partly to the portability, broad availability, and improved technology of ultrasound machines and their practical utility as diagnostic, therapeutic, monitoring, and procedural-guidance tools. Moreover, higher-resolution ultrasound devices have become available for operating rooms, postanesthesia care units, intensive care units, and perioperative clinics.[3,4] As a consequence, proficiency in echocardiography and LUS now is considered necessary for the anesthesiologist and the intensivist and has therefore been implemented in many residency and fellowship curricula.[5-9]

M-mode (motion-based) ultrasonographic imaging can be better understood by describing the multiple ultrasound modalities that have been developed as technology has evolved. A-mode (amplitude-based) imaging displays the reflected echoes as peaks on an oscillator monitor, and B-mode (brightness-based) imaging converts A-mode spikes to dots whose brightness matches signal intensity. Today, these 2 modalities are rarely used in the clinical domain. M-mode imaging includes a time scale, whereby reflected echoes displayed in B-mode along a single line on the vertical axis are placed side by side on the horizontal axis, representing their motion toward and away from the transducer over time. M-mode is therefore ideal for the evaluation of motion and timing. M-mode–derived parameters generally require simple linear measurements from single recordings through standard windows. The slowest M-mode frame rate (at least 1,000 frames per second) is 10 times greater than the fastest 2-dimensional (2D) ultrasonography image (≈100 frames per second). This higher sampling rate affords M-mode the best temporal resolution among ultrasound modalities, which makes it ideal for evaluating very fast or subtle movements, such as those of the cardiac valves or the inferior vena cava (IVC), respectively. Furthermore, conventional M-mode image quality does not depend on 2D image quality but on tissue acoustic characteristics and pulse repetition frequency.[10]

Although A-mode and B-mode were the first ultrasound modalities described, M-mode provided the first ultrasonographic images of the moving heart in 1953, as published by Inger Edler and Hertz.[11,12] In the United States, Harvey Feigenbaum would later refine M-mode imaging for measurement of heart chamber dimensions. M-mode was then the leading echocardiographic modality for approximately 10 years until 2D and Doppler techniques were developed. Since then, M-mode echocardiography has been progressively abandoned and now is seldomly used in many practices.[13] In contrast, part of the global success of LUS can be attributed to M-mode imaging. Although in his first report in 1992 Daniel Lichtenstein used mainly 2D imaging, he would later use M-mode recordings extensively to characterize many of the fundamental signs in LUS.[12] Today, conventional M-mode parameters are used in standard LUS evaluations, and novel parameters are being investigated actively.

For the anesthesiologist and the critical care physician, comprehensive echocardiographic measurements often are time-consuming and technically challenging, and 2D images in LUS do not permit evaluation of subtle movements that may be clinically relevant. Rapid and practical measurements in critical care and anesthesia allow for early and serial evaluations during the evolution of a patient's clinical course. M-mode recordings provide accurate estimates of hemodynamicsand cardiopulmonary status, as well as therapeutic and procedural guidance in a timely and practical fashion. Hence, the authors of the present review believe that M-mode is a valuable tool for assessing critically ill and surgical patients and thus M-mode imaging should remain active in daily practice while being continually investigated for novel applications.

This article aims to comprehensively review contemporary applications of M-mode ultrasonography in the practice of anesthesia and critical care medicine. For each clinical application, the following are provided: definitions, technical descriptions for image acquisition and interpretation, evidence-based clinical implications in critically ill and surgical patients, and associated limitations. In this article, the measurements with respective clinical applications reviewed are left ventricular (LV) function (mitral annular plane systolic excursion [MAPSE], E-point septal separation [EPSS], LV fractional shortening [LVFS], and transmitral propagation velocity); followed by right ventricular (RV) function (tricuspid annular plane systolic excursion [TAPSE], subcostal echocardiographic assessment of tricuspid annulus kick [SEATAK], RV outflow tract [RVOT] FS, motion of the ventricular septum [VS], RV wall thickness, and RVOT obstruction); and then volume status and responsiveness (IVC and superior vena cava [SVC] diameter and respiratory variability [collapsibility and distensibility indexes]); cardiac tamponade; systolic anterior motion (SAM) of the mitral valve; and aortic dissection. Table 1 provides a summary of abnormal cutoff values for quantitative M-mode echocardiographic parameters (Fig. 1-10).

Technical Considerations

Current international guidelines recommend synchronizing imaging with electrocardiographic tracings as a minimum quality standard for echocardiography and suggest the use of respirometry recording whenever possible.[14-16] For M-mode imaging, temporal correlation between cardiopulmonary events and cardiac and respiratory cycles is fundamental for adequate image interpretation and clinical correlation. Most ultrasound devices used by critical care physicians and anesthesiologist have capabilities for electrocardiography and respirometry recordings, although connection of electrocardiography cables and chest wall pads may be inconvenient in emergency situations, and recordings can be unstable and vary depending on patient positioning. Moreover, small, portable ultrasound machines may not have this capability.

Because M-mode depicts motion of structures along the vertical axis, optimal M-mode–derived measurements require parallel alignment between the axis of the ultrasonic beam (M-mode vector) and the axis of the motion of the structure of interest, a task that sometimes is technically impossible. Nonetheless, this limitation can be overcome by the use of anatomic M-mode. Anatomic M-mode uses 2D images as a basis for

Table 1
Summary of Abnormal Cutoff Values for Quantitative M-Mode Echocardiographic Parameters

Parameter	Abnormal Cutoff Value	Illustrative Echocardiographic View
Left ventricular function		
MAPSE	<10 mm	Fig 1
EPSS	>7 mm	Fig 2
LVFS, endocardial	<27%*	-
	<25%†	
LVFS, midwall	<15%*	Fig 3
	<14%†	
Vp	<56 cm/s	Fig 4
Vp/Ap	<1.06	-
Right ventricular function		
TAPSE	<17 mm	Fig 5
RVOT FS	<32%	Fig 7
RVWT	>5 mm	-
Volume status and responsiveness		
End-expiratory IVCd	≤1.3 cm‡	Fig 9
	≥2.5 cm§	
IVC collapsibility index¶	>40%-42%‡,‖	Fig 9
	>48%‡,#	
IVC distensibility index**	>18%‡	Fig 9
IVCd variation index††	>12%‡	Fig 9
SVC collapsibility index‡‡	>36%‡	Fig 10

Abbreviations: EPSS, E-point septal separation; IVC, inferior vena cava; IVCd, inferior vena cava diameter; IVCd-max; maximum inferior vena cava diameter; IVCd-min, minimum inferior vena cava diameter; LVFS, left ventricular fractional shortening; MAPSE, mitral annular plane systolic excursion; RVOT FS, right ventricular outflow tract fractional shortening; RVWT, right ventricular wall thickness; SVC, superior vena cava; SVCd-max; maximum superior vena cava diameter; SVCd-min, minimum superior vena cava diameter; TAPSE, tricuspid annular plane systolic excursion; Vp, early propagation velocity; Vp/Ap, early-to-late propagation velocity ratio.

* For women.

† For men.

‡ Fluid responsiveness.

§ Fluid unresponsiveness.

¶ IVC collapsibility index = IVCd-max − IVCd-min/IVCd-max.

‖ IVC collapsibility index after spontaneous breathing technique.

IVC collapsibility index after standardized breathing technique.

** IVC distensibility index = IVCd-max − IVCd-min/IVCd-min.

†† IVCd variation index = IVCd-max − IVCd-min/0.5(IVCd-max + IVCd-min).

‡‡ SVC collapsibility index = SVCd-max − SVCd-min/SVCd-max.

M-mode analysis at a defined line, whereby it allows for adjusting the orientation of the M-mode vector, regardless of transducer orientation, to place it as parallel as possible to the direction of motion of the structure of interest.[17] This modality, however, may not be available in small, portable ultrasound machines and has considerable limitations, including lower image resolution and, consequently, less-accurate measurements.

Left Ventricular Function

Mitral Annular Plane Systolic Excursion

Annular or longitudinal displacement is an essential property of LV function.[18] MAPSE, also referred to as mitral annular excursion or displacement, is a simple and well-validated M-mode–derived marker of summative LV longitudinal function and is closely correlated with global LV function.[19] Although MAPSE has been used as a prognostic factor for major cardiac events in patients with cardiovascular disease, its application was eclipsed quickly by the introduction of Doppler imaging.[20-22] MAPSE can be useful in urgent clinical decision-making in the critical care and anesthesia settings because of its limited dependence on image quality, easy acquisition, and accuracy in prediction of LV function.[23,24]

Technique

MAPSE is obtained using the standard apical 4-chamber view (transthoracic echocardiography [TTE]) or the midesophageal 4-chamber view (transesophageal echocardiography [TEE]) with the M-mode vector placed through both the septal and lateral mitral annuli (see Fig 1, A and B). The systolic excursion of the septal and lateral mitral annuli then is measured from the lowest (end-diastole) to the highest (end-systole) points; the 2 are measured in millimeters and averaged.[23] With TEE, care is needed to avoid foreshortening and to include as much of the full length of the LV as possible, especially the apex.

Clinical Implications

A MAPSE value ≥10 mm indicates preserved left ventricular ejection fraction (LVEF) (≥55%), with a sensitivity of 92% and a specificity of 87% in patients with symmetrical LV morphology and overall normal wall motion, whereas a MAPSE value <8 mm is associated with decreased LVEF (<50%), with a specificity of 82% and a sensitivity of 98% (see Fig 1, B and C).[25,26] Of note, MAPSE also is well-correlated with diastolic echocardiographic parameters such as e′ and E/e′, even in patients with sepsis or heart failure with preserved LVEF.[19,27-29] In addition, in patients with shock, MAPSE is correlated with myocardial injury biomarkers (high-sensitive troponin), and, unlike LVEF, it is an independent predictor of 28-day mortality.[27] Furthermore, a MAPSE value <10 mm portends worse long-term outcome in patients with Takotsubo cardiomyopathy.[30] Lastly, MAPSE correlates well with LV longitudinal strain, a sensitive, earlier marker of cardiac dysfunction that is not widely available in the operating room or critical care setting and has its own technical difficulties.[31]

Because MAPSE shows considerable variation due to cardiac size, especially in children, Terada et al.[32] developed a simple, age-adjusted parameter in which MAPSE is divided by LV long-axis length (MAPSE/L). LV long-axis length is measured with TTE on the apical 4-chamber view as the distance between the lateral mitral annulus and the endocardial border of the LV apex at end-diastole. Normal values were established, and, in all cases beyond the neonatal period until age 15 years, MAPSE/L was significantly associated with age, LV global longitudinal strain, and LVEF.

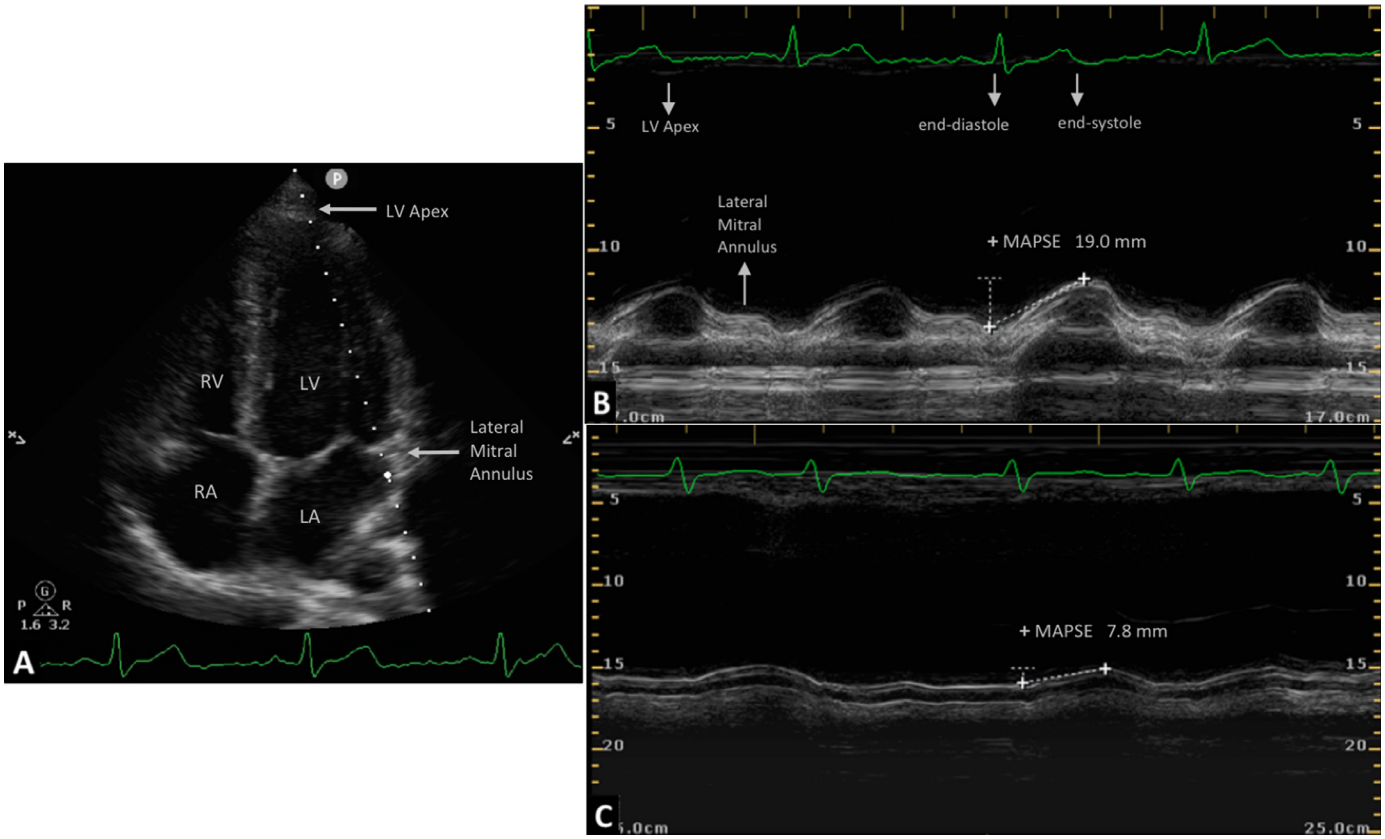

Fig 1. Mitral annular plane systolic excursion by transthoracic echocardiography. (A) Two-dimensional image of apical 4-chamber view describing the image acquisition before M-mode imaging of mitral annular plane systolic excursion; the M-mode line (*white dotted line*) is placed through the left ventricular apex (*upper arrow*) and the lateral mitral annulus (*lower arrow*); then, M-mode imaging can be recorded. (B) M-mode image of normal mitral annular plane systolic excursion (19.0 mm) suggesting normal left ventricular systolic function. The left ventricular apex (*upper left arrow*) and the lateral mitral annulus (*lower arrow*) are depicted across several cardiac cycles. Mitral annular plane systolic excursion is measured as the vertical excursion of the lateral mitral annulus from end-diastole to end-systole (electrocardiographic points indicated by *upper mid and right arrows*, respectively). (C) M-mode image of abnormal mitral annular plane systolic excursion (7.8 mm) suggesting left ventricular systolic dysfunction. LA, left atrium; LV, left ventricle; MAPSE, mitral annular plane systolic excursion; RA, right atrium; RV, right ventricle.

Limitations

MAPSE, like other several parameters described in this article, was initially developed and validated in TTE and then extrapolated to TEE; thus, most of the evidence focuses on TTE. Large studies that have evaluated the accuracy and feasibility of MAPSE by TEE are lacking.

Like most of the echocardiographic parameters of LV systolic function that account for contractility, MAPSE is preload dependent, at least as much as LVEF.[27,33] MAPSE does not account for segmental LV function; thus, in patients with focal myocardial dysfunction, such as regional wall motion abnormalities, small areas of fibrosis, or conduction disorders, MAPSE measurements may not correlate well with LV function. Also, in patients with LV hypertrophy, mitral valve calcification, and chronic atrial fibrillation, MAPSE may not be reliable.[19,20,34] It must be emphasized that these conditions are particularly common among patients in the intensive care unit (ICU). MAPSE also may not be reliable in patients with increased translational motion of the heart, such as cases of mobile apex due to large pericardial effusion.[32] Moreover, after cardiac surgery, septal MAPSE, together with RV function, might be more decreased compared with lateral MAPSE.[19] Finally, with increasing age, MAPSE is progressively decreased, whereas LVEF remains unchanged or slightly increased; this phenomenon has shown that MAPSE could overestimate LV function in young patients.[35,36]

E-Point Septal Separation

In early diastole the mitral valve leaflets separate widely, with a maximum motion of the anterior leaflet toward the VS. The narrowest distance between the anterior valve leaflet and the VS is defined as the EPSS and has long been correlated with LV systolic function.[37,38]

Technique

EPSS is obtained by TTE using the parasternal long-axis view.[39] The M-mode vector is placed through the tip of the

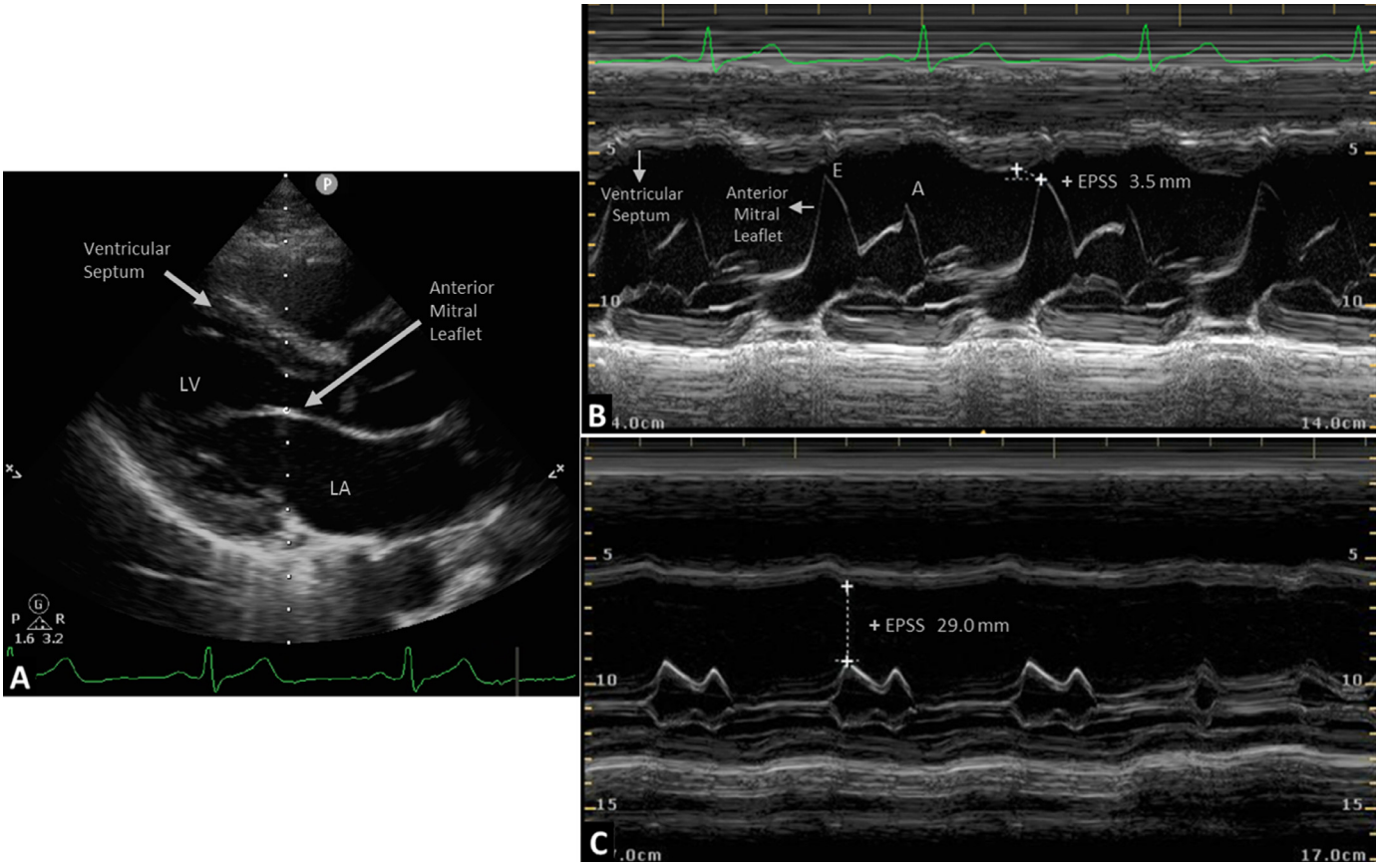

Fig 2. E-point septal separation by transthoracic echocardiography. (A) Two-dimensional image of parasternal long-axis view describing the image acquisition before M-mode imaging of E-point septal separation; the M-mode line (*white dotted line*) is placed through the ventricular septum (*upper arrow*) and the tip of the anterior mitral leaflet (*lower arrow*); then, M-mode imaging can be recorded. (B) M-mode image of normal E-point septal separation (3.5 mm) suggesting normal left ventricular systolic function. The ventricular septum (*upper vertical arrow*) and the anterior mitral leaflet (*lower horizontal arrow*) are depicted across several cardiac cycles. "E" indicates the early opening of the anterior mitral leaflet caused by early diastolic filling; "A" corresponds to the late opening of the anterior mitral leaflet caused by atrial contraction during late diastolic filling. E-point septal separation is measured as the distance between the anterior mitral leaflet and ventricular septum at early diastole (ie, at "E"). (C) M-mode image of abnormal E-point septal separation (29.0 mm) suggesting left ventricular systolic dysfunction. EPSS, E-point septal separation; LA, left atrium; LV, left ventricle.

anterior leaflet of the mitral valve, and only 1 linear measurement is required (see Fig 2, A and B).[10]

Clinical Implications

An EPSS value >7 mm has been universally accepted as a marker of severe LV systolic dysfunction (LVEF <30%) (see Fig 2, C).[37,40-43] In a recent study,[44] this cutoff value showed a sensitivity of 100% for predicting severe LV systolic dysfunction in patients with calculated LVEF, but the specificity was low (51%). In contrast, that study found only a moderate correlation between "eyeballing" estimates of LV systolic function and calculated LVEF. EPSS is well-correlated with angiography, cardiac magnetic resonance imaging, visual estimation ("eyeballing"), and quantitative echocardiographic imaging (Simpson's method) for assessment of LVEF in various cardiac conditions, including myocardial infarction, left bundle branch block (LBBB), paradoxical septal motion, regional wall–motion abnormalities, and aortic stenosis.[37,40-43,45]

Limitations

Valvular pathologic processes that restrict the motion of the anterior mitral leaflet toward the VS, such as mitral stenosis, mitral annulus calcification, and moderate to severe aortic regurgitation, can lead to an exaggerated EPPS, yielding an underestimated LV function.[45] Moreover, severe LV hypertrophy, asymmetric septal hypertrophy, and discrete proximal septal thickening (sigmoid VS) can lead to falsely small EPSS measurements and thus overestimate LV systolic function.[41,42] In ICU patients, the image quality required for EPSS measurement often is difficult to achieve, and if the measurement is not made on an appropriate parasternal long-axis view (ie, horizontal orientation of the heart with both the mitral and aortic valves clearly seen in the same frame), the EPSS may be overestimated because of a tangential measurement.

Left Ventricular Fractional Shortening

LVFS measures the ratio or percentage of LV diameter change from diastole to systole. Calculation of LVFS implies

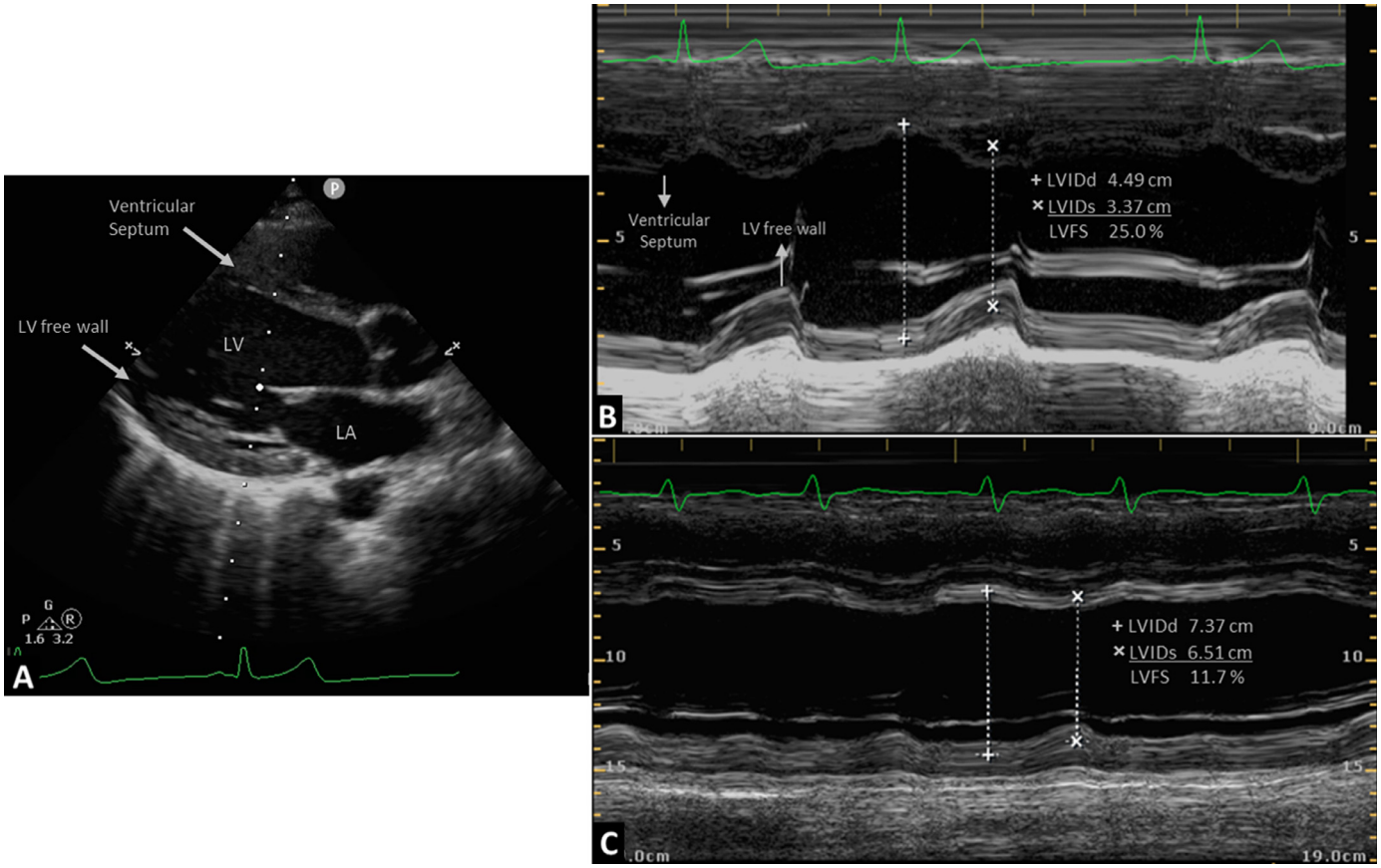

Fig 3. Midwall left ventricular fractional shortening by transthoracic echocardiography. (A) Two-dimensional image of parasternal long-axis view describing the image acquisition before M-mode imaging of midwall left ventricular fractional shortening; the M-mode line (*white dotted line*) is placed through the ventricular septum (*upper arrow*, passing below the tip of the anterior mitral leaflet) and the left ventricular free wall (*lower arrow*); then, M-mode imaging can be recorded. (B) M-mode image of normal midwall left ventricular fractional shortening (25.0%) suggesting normal left ventricular systolic function. The ventricular septum (*upper arrow*) and the left ventricular free wall (*lower arrow*) are depicted across several cardiac cycles. (C) M-mode image of abnormal midwall left ventricular fractional shortening (11.7%) suggesting left ventricular systolic dysfunction. LA, left atrium; LV, left ventricle; LVFS, left ventricular fractional shortening; LVIDd, left ventricular internal diameter at end-diastole; LVIDs, left ventricular internal diameter at end-systole.

that the measurements are taken at a plane related to the chamber's maximal (diastolic) and subsequent minimal (systolic) dimensions throughout a cardiac cycle.

Technique

LVFS can be derived either by TTE using the parasternal long-axis view or TEE using the transgastric short-axis view, with the M-mode vector placed below or at the tips of the anterior mitral leaflet (see Fig 3, A and B), and then measuring the percentage decrease in LV end-diastolic diameter that occurs by end-systole, as follows:

$$\text{LVFS} = \text{LVIDd} - \text{LVIDs}/\text{LVIDd} \times 100$$

where LVIDd is LV internal diameter at end-diastole and LVIDs is LV internal diameter at end-systole.[10,46,47] The midwall LVFS is preferred over the endocardial LVFS because it reflects both the inward motion of the endocardium and the degree of wall thickening (see Fig 3, B). The parasternal short-axis view is considered as an alternative view to obtain LVFS.[10,48]

Clinical Implications

Endocardial LVFS <27% for women and <25% for men and midwall LVFS <15% for women and <14% for men are considered markers of LV dysfunction (see Fig 3, C).[10,49] LVFS is useful for detecting LV systolic dysfunction, especially in patients with LV concentric hypertrophy.[50] Interestingly, unlike endocardial FS, subnormal midwall LVFS also has been correlated with LV diastolic dysfunction.[51]

Increased or hyperdynamic LV function can be recognized by a qualitative evaluation of the systolic radial inward motion of the LV walls on the parasternal short- or long-axis view. Hyperdynamic LV function is defined as near or complete obliteration of the LV cavity, meaning that the endocardial surfaces of the LV free wall and septum come in close contact with each other.[52] In patients with nontraumatic undifferentiated shock, hyperdynamic LV function predicts sepsis as the cause of shock with a specificity of 94%.[53] In this patient population, the hyperdynamic LV function is accompanied by a normal LV end-diastolic area or volume. In contrast, in severely hypovolemic patients, hyperdynamic LV function

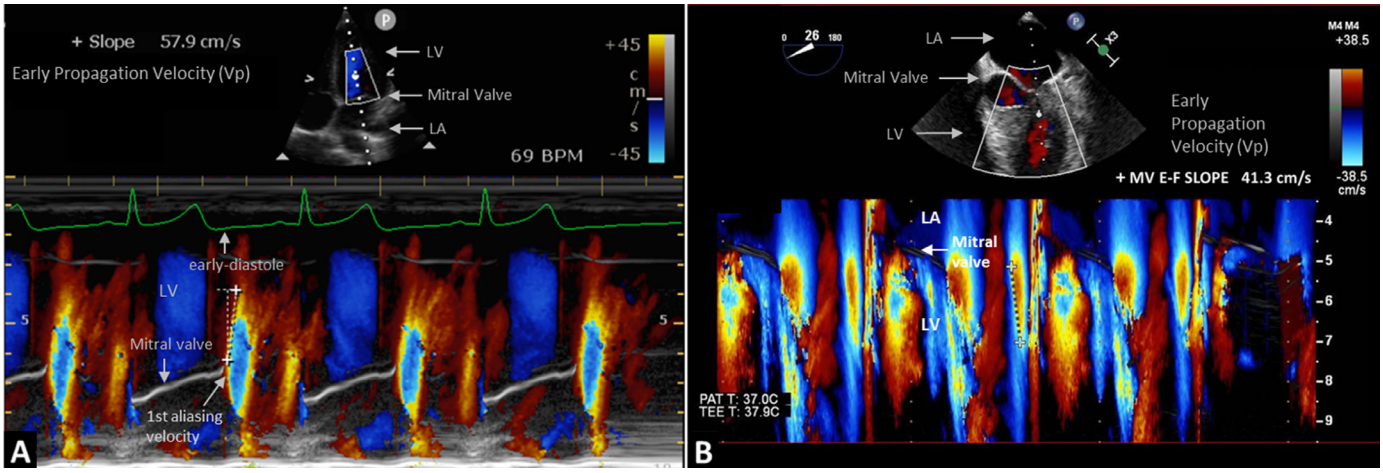

Fig 4. Early propagation velocity by transthoracic and transesophageal echocardiography. (A) Color M-mode image of normal propagation velocity (57.9 cm/s) by transthoracic echocardiography suggesting normal left ventricular diastolic function. At the top, 2-dimensional image of apical 4-chamber view with the M-mode line (*white dotted line*) placed through the left ventricle (*upper arrow*), mitral valve (*middle arrow*), and left atrium (*lower arrow*) and the color Doppler interrogation field located from the mitral valve and distally into the left ventricle. At the bottom, color M-mode image of blood flow from the mitral valve (*lower left arrow*) to the left ventricle at early diastole (*upper arrow* indicates corresponding electrocardiographic point). Propagation velocity is measured as the slope of the first aliasing velocity (*lower right arrow*) from the mitral valve plane to 4 cm into the left ventricle at early diastole. (B) Color M-mode image of abnormal propagation velocity (41.3 cm/s) by transesophageal echocardiography suggesting left ventricular diastolic dysfunction. At the top, 2-dimensional image of midesophageal 4-chamber view with the M-mode line (*white dotted line*) placed through the left atrium (*upper arrow*), mitral valve (*middle arrow*), and left ventricle (*lower arrow*) and the color Doppler interrogation field located from the mitral valve and distally into the left ventricle. At the bottom, color M-mode imaging of blood flow from the left atrium through mitral valve (*arrow*) to the left ventricle at early diastole. LA, left atrium; LV, left ventricle.

could be present but with a reduced LV end-diastolic area or volume.

Limitations

In patients with an asymmetrically enlarged left ventricle or with regional wall motion abnormalities due to coronary artery disease or conduction abnormalities, LVFS may not correlate well with the actual global LV function.[54] Furthermore, sudden changes in afterload and preload can alter LVFS measurements.

Color M-Mode Transmitral Propagation Velocities

Color M-mode (CMM) echocardiographic assessment of transmitral flow is a reliable parameter of LV diastolic function not affected by the atrioventricular pressure gradient, active relaxation and distensibility of the LV, or preload conditions.[55,57] CMM provides information in a spatiotemporal fashion by combining color Doppler and M-mode imaging in real time. CMM imaging represents all multiple simultaneous color-pixel Doppler tracings acquired at different levels, from mitral valve to apical areas.

Technique

Using the apical 4-chamber view (TTE) or the midesophageal 4-chamber view (TEE), with visualization of the entire LV long axis and highest sweep speed, the M-mode vector is placed through the center of the mitral inflow, and a color Doppler interrogation sample is located from the mitral valve and distally into the LV cavity, where it is used to evaluate mitral-to-apex inflow during diastole (see Fig 4, A and B).[56,57]

Clinical Implications

Early propagation velocity (Vp) is measured as the slope of the first aliasing velocity (40-45 cm/s) from the mitral valve plane at early diastole to 4 cm into the left ventricle. Vp is a reliable index of LV relaxation in patients with decreased LVEF and a dilated left ventricle, but not in patients with normal LVEF.[58] Indeed, Vp allows for the identification of delayed relaxation or a pseudonormal filling pattern that is not recognized with pulsed-wave Doppler evaluations (E-wave velocity).[56,59] Abnormal Vp values are also correlated with acute myocardial infarction and its long-term outcomes.[57,60] Normal Vp values are >55 cm/s in younger adults and >45 cm/s in older adults.[61] In one series, a cutoff value of 56 cm/s separated a normal from a pseudonormal filling pattern with a sensitivity of 92% and specificity of 98% (see Fig 4, A and B).[62]

The ratio of early-to-late propagation velocities (Vp/Ap), although less studied than Vp alone, appears to be a reliable diastolic index regardless of systolic function and is of particular utility in patients with delayed relaxation or pseudonormal filling pattern.[62,63] A cutoff value of 1.06 separates normal from pseudonormal filling pattern with a sensitivity of 98% and specificity of 100%.[62]

Because diastolic dysfunction is characterized by a reduction in both initial Vp and the distance to the deceleration point (occurring closer to the mitral annulus), the product of these 2 parameters, termed Vs, may provide a more accurate evaluation of diastolic dysfunction than does

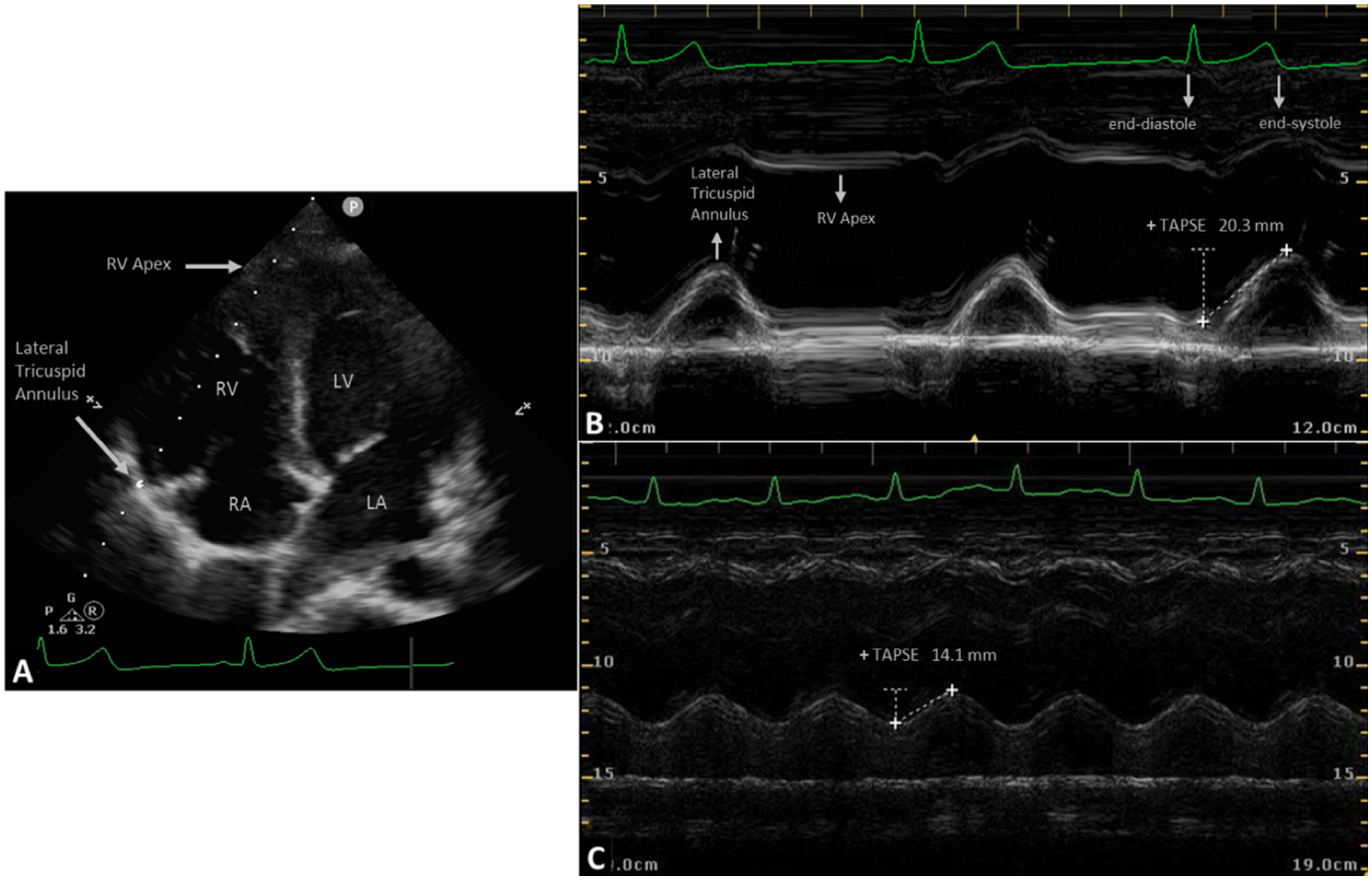

Fig 5. Tricuspid annular plane systolic excursion by transthoracic echocardiography. (A) Two-dimensional image of apical 4-chamber view describing the image acquisition before M-mode imaging of tricuspid annular plane systolic excursion; the M-mode line (*white dotted line*) is placed through the right ventricular apex (*upper arrow*) and the lateral tricuspid annulus (*lower arrow*); then, M-mode imaging can be recorded. (B) M-mode image of normal tricuspid annular plane systolic excursion (20.3 mm) suggesting normal right ventricular function. The lateral tricuspid annulus (*lower arrow*) and the right ventricular apex (*middle arrow*) are depicted across several cardiac cycles. Tricuspid annular plane systolic excursion is measured as the vertical excursion of the lateral tricuspid annulus from end-diastole to end-systole (electrocardiographic points indicated by *upper left* and *right arrows*, respectively). (C) M-mode image of abnormal tricuspid annular plane systolic excursion (14.1 mm) suggesting right ventricular dysfunction.

LA, left atrium; LV, left ventricle; RA, right atrium; RV, right ventricle; TAPSE, tricuspid annular plane systolic excursion.

conventional Vp alone. Vs represents the strength of the initial inflow propagation and the magnitude of LV suction. Vs is particularly useful in patients with hypertrophic cardiomyopathy (HCM), where it was found to be more reliable than Vp alone in diagnosing diastolic dysfunction. A Vs value <199 cm^2/s identifies a reduced intraventricular pressure gradient (<2.2 mmHg), and a Vs value <155 cm^2/s detects increased pulmonary capillary wedge pressure (>18 mmHg).[64]

The combination of conventional transmitral flow parameters (eg, E velocity) with CMM parameters (eg, Vp, Vp/Ap, Vs) has provided more accurate estimates of left atrial pressure. The index E/Vp correlates well with the pulmonary capillary wedge pressure in adults with normal or decreased LVEF or with acute myocardial infarction.[58,65,66]

Limitations

The reliability of Vp is compromised if there are variations in the degree of LV relaxation (eg, atrial fibrillation), LV geometry, or mitral orifice size.[59,62,67,68] Moreover, there is controversy about whether Vp is a reliable index of diastolic function in patients with HCM.[59,69] Compared with CMM, tissue Doppler imaging provides comparable information regarding LV diastolic function but in a simpler and more reproducible fashion. However, tissue Doppler imaging requires advanced machine capability that may not be available in some ICUs. Table 2 provides a summary of the M-mode echocardiographic parameters of LV function.

Right Ventricular Function

As a low-pressure, high-volume, thin-walled structure, the right ventricle has particular anatomic and physiological considerations that the echocardiographer must account for when examining with M-mode.[69] The right ventricle takes an anterior course to the left ventricle, leading to a crescent shape composed of the following 3 distinct anatomic regions: inflow, apical trabecular, and outflow.[70]

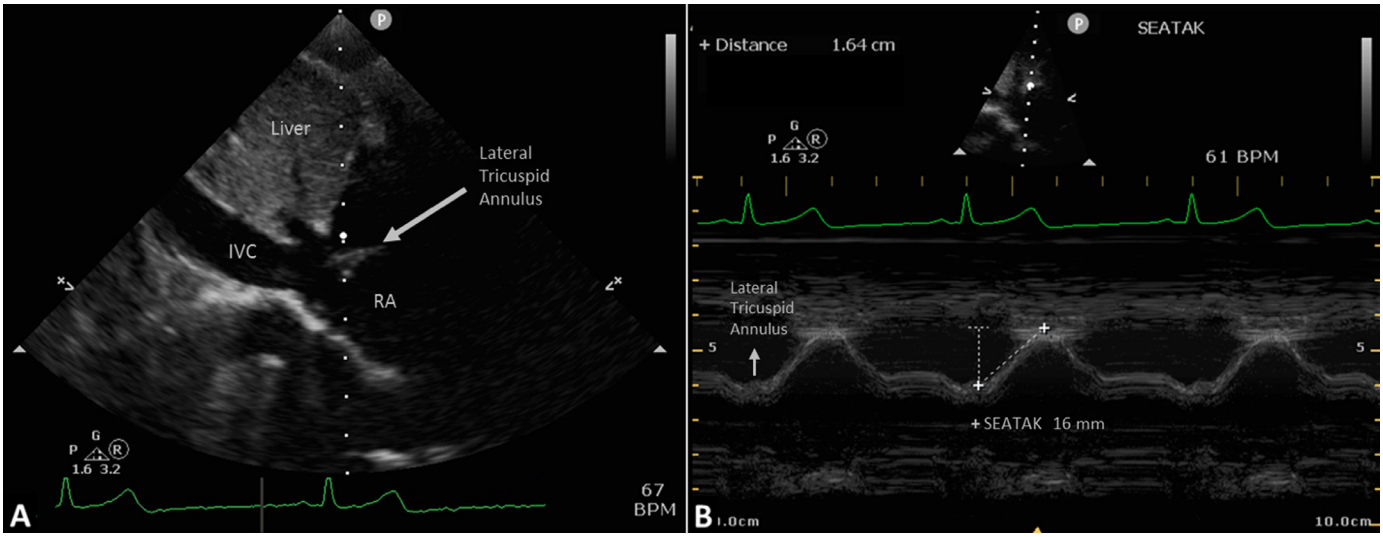

Fig 6. Subcostal echocardiographic assessment of tricuspid annulus kick by transthoracic echocardiography. (A) Two-dimensional image of subcostal window, inferior vena cava view describing the image acquisition before M-mode imaging of subcostal echocardiographic assessment of tricuspid annulus kick; the M-mode line (*white dotted line*) is placed through the lateral tricuspid annulus (*arrow*); then, M-mode imaging can be recorded. (B) M-mode image of the subcostal echocardiographic assessment of tricuspid annulus kick measurement (16 mm). The lateral tricuspid annulus (*arrow*) is depicted across several cardiac cycles. The subcostal echocardiographic assessment of tricuspid annulus kick is measured as the vertical excursion of the lateral tricuspid annulus from end-diastole to end-systole. IVC, inferior vena cava; RA, right atrium; SEATAK, subcostal echocardiographic assessment of tricuspid annulus kick.

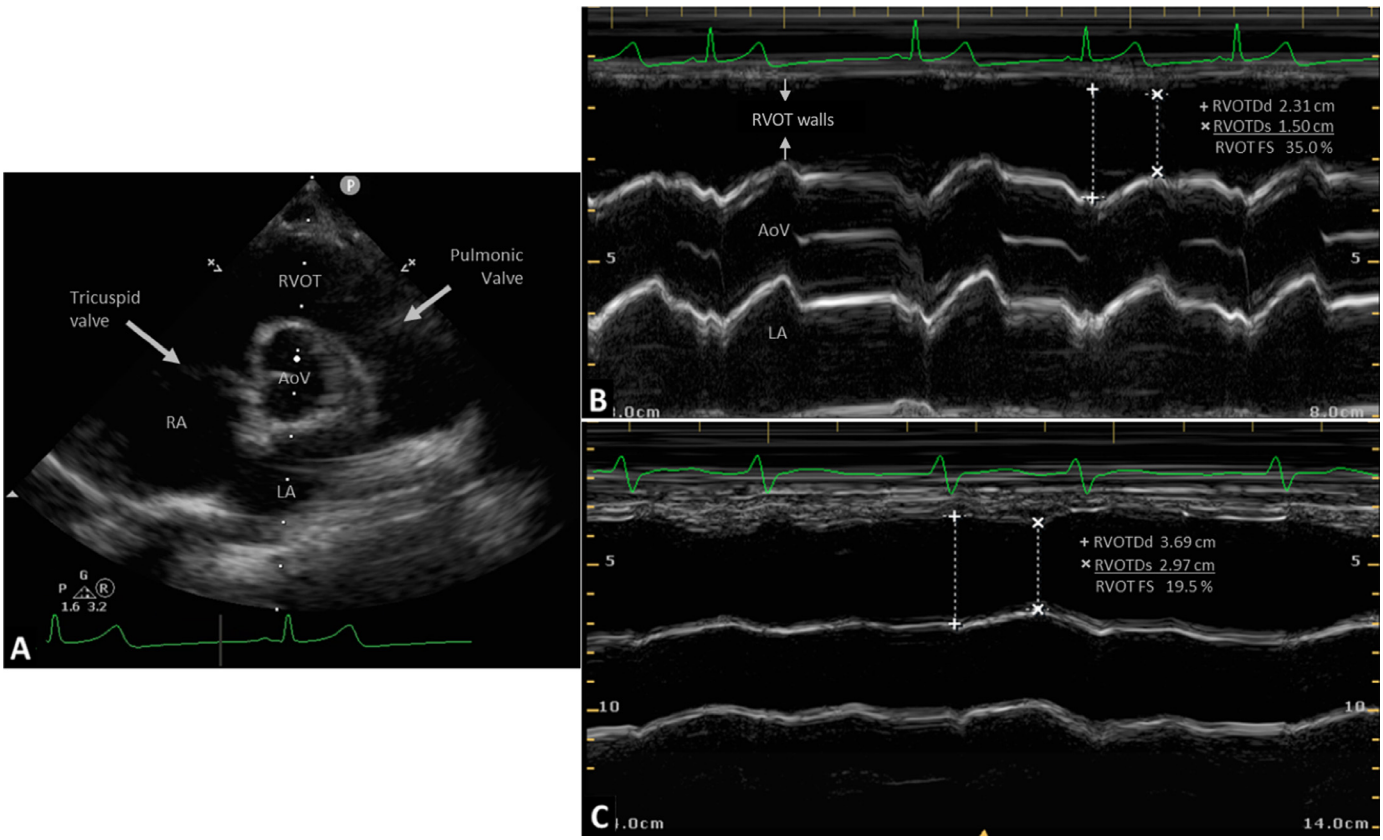

Fig 7. Right ventricular outflow tract fractional shortening by transthoracic echocardiography. (A) Two-dimensional image of parasternal short-axis view, aortic valve level describing the image acquisition before M-mode imaging of right ventricular outflow tract fractional shortening; the M-mode line (*white dotted line*) is placed through the right ventricular outflow tract, aortic valve, and left atrium; then, M-mode imaging can be recorded. The right atrium, tricuspid valve (*left arrow*), and pulmonary valve (*right arrow*) also are seen. (B) M-mode image of normal right ventricular outflow tract fractional shortening (35.0%) suggesting normal right ventricular function. The right ventricular outflow tract walls (*arrows*), aortic valve, and left atrium are depicted across several cardiac cycles. (C) M-mode image of abnormal right ventricular outflow tract fraction shortening (19.5%) suggesting right ventricular dysfunction. AoV, aortic valve; LA, left atrium; RA, right atrium; RVOT, right ventricular outflow tract; RVOT FS, right ventricular outflow tract fractional shortening; RVOTDd, RVOT diameter at end-diastole; RVOTDs, RVOT diameter at end-systole.

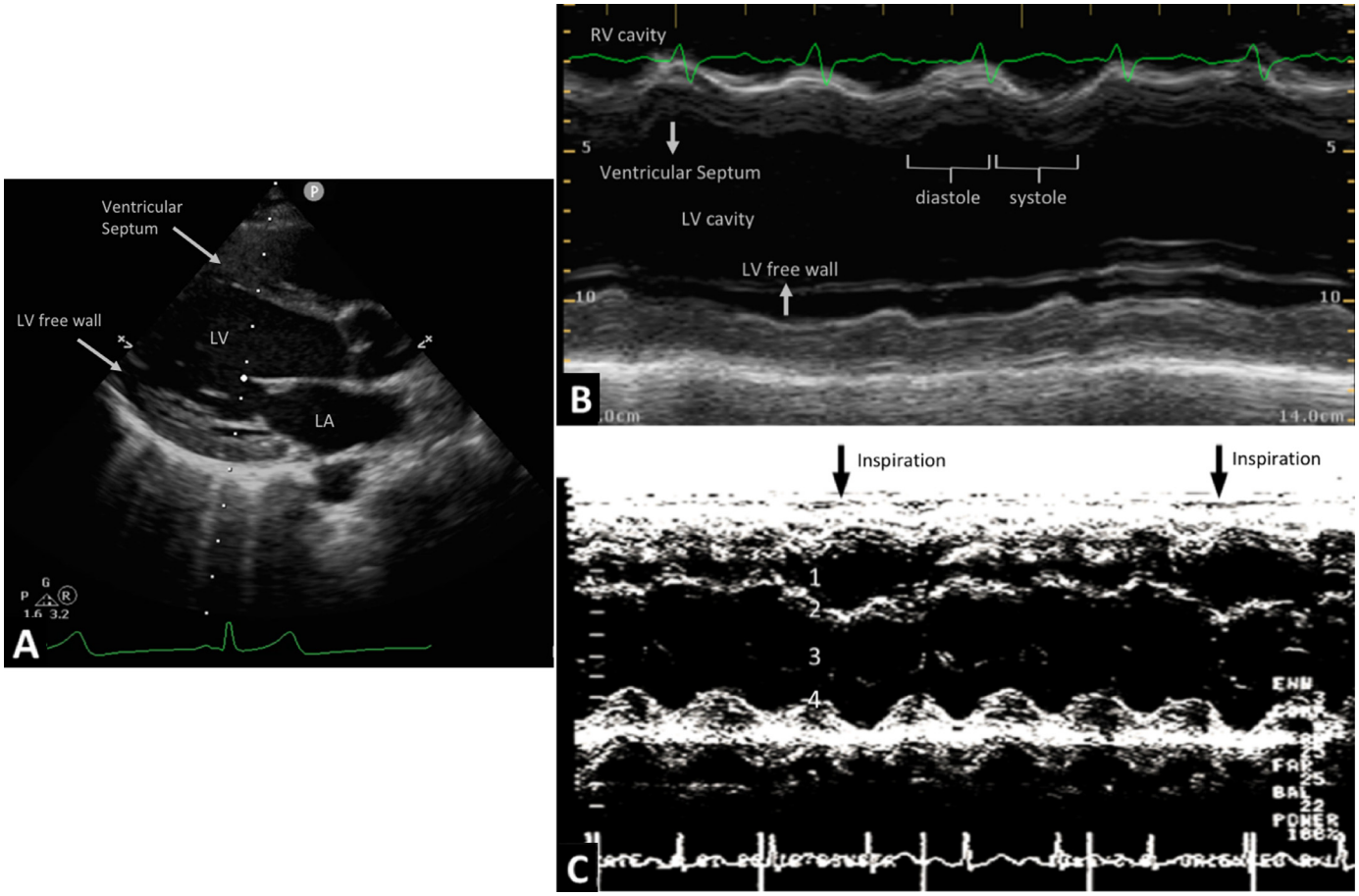

Fig 8. Motion of the ventricular septum by transthoracic echocardiography. (A) Two-dimensional image of parasternal long-axis view, describing the image acquisition before M-mode imaging of the ventricular septum; the M-mode line (*white dotted line*) is placed across the right ventricular outflow tract and below the tips of the anterior mitral leaflet; then, M-mode imaging can be recorded. (B) M-mode image of normal motion of the ventricular septum. From top to bottom, right ventricular cavity, ventricular septum (*upper arrow*), left ventricular cavity, and left ventricular free wall (*lower arrow*). During diastole (*left bracket*), the ventricular septum thins and moves rightward (toward the right ventricle); during systole (*right bracket*), the ventricular septum thickens and moves leftward (toward the left ventricle). (C) M-mode image of abnormal motion of the ventricular septum in a patient with severe asthma. From top to bottom, right ventricular cavity *(1)*, ventricular septum *(2)*, left ventricular cavity *(3)*, and left ventricular free wall *(4)*. During inspiration (*arrows*), there is leftward shift (toward the left ventricular cavity) and flattening of the ventricular septum as a major contributor to the transitory decrease in left ventricular cardiac output during inspiration (ie, pulsus paradoxus). RVOT, right ventricular outflow tract; VS, ventricular septum;

Physiologically, the contractile mechanism is initiated in the inlet, with a systolic ejection movement toward the apex, followed by sequential contributions from the free wall, outflow, and ventricular septum anatomic regions.[69] This contractile apparatus faces an afterload resultant from pulmonary vascular resistance and impedance, physiological forces that can influence shaping of anatomic structures with subsequent echocardiographic sequelae.[69] The literature has described the echocardiographic imaging of the right ventricle to be challenging because of its shape, position, and thin-walled structure; however, the importance of perioperative imaging can be appreciated in several surgical populations at high risk for RV failure, including patients with a ventricular assist device and pulmonary hypertension and those who have undergone lung transplantation.[69-73] Evaluation of the right ventricle, whether measuring contractility or effects of afterload changes, can be accomplished using M-mode imaging.

Right Ventricular Contractility

Tricuspid Annular Plane Systolic Excursion

RV myocardial contraction in the longitudinal plane accounts for the vast majority (80%) of the global RV systolic function. Hence, TAPSE, also referred to as tricuspid annular motion, is a well-validated, M-mode–derived parameter that represents the RV longitudinal function.[74,75] TAPSE is well-correlated with parameters of global RV systolic function, such as radionuclide-derived RV ejection fraction, RV fractional area change, and RVEF by the Simpson's method.[76-78] Similarly to MAPSE, TAPSE is rapidly obtained and interpreted, has good intraobserver and interobserver reliability, and has little dependence on image quality and endocardial resolution.[75] Also, TAPSE by TTE has been shown to be the least user-dependent measure of RV performance.[74,79]

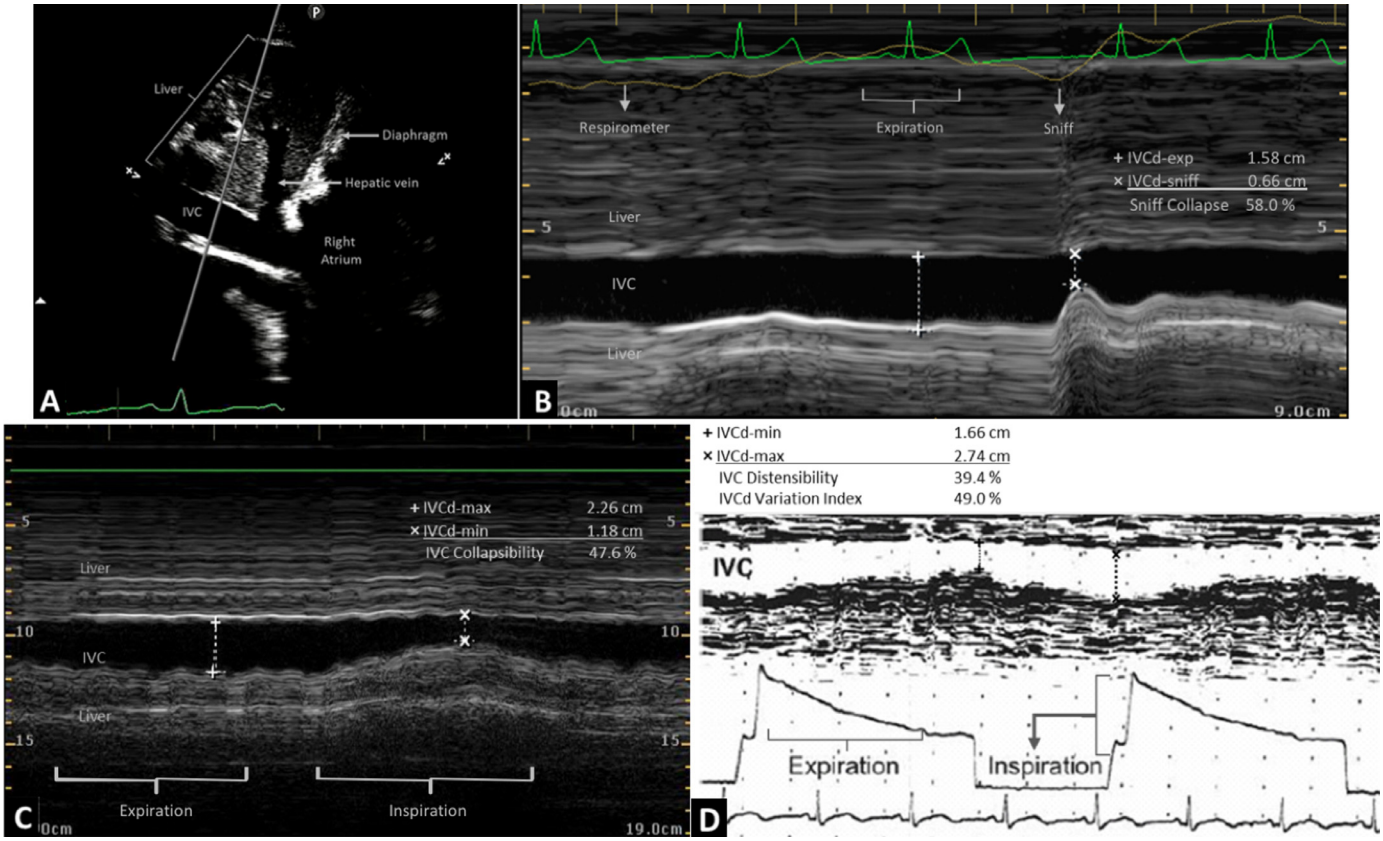

Fig 9. Inferior vena cava assessment by transthoracic echocardiography. (A) Two-dimensional image of subcostal window, inferior vena cava view describing the image acquisition before M-mode imaging of the inferior vena cava; the M-mode line (*gray line*) is placed across the inferior vena cava, 2 to 3 cm before its entry to the right atrium; then, M-mode imaging can be recorded. The diaphragm (*upper arrow*) and hepatic vein (*lower arrow*) also are seen. (B) M-mode image of inferior vena cava diameter (IVCd) of 1.58 with a collapsibility of 58.0% after sniff test, suggesting right atrial pressure of 3 mmHg. Inferior vena cava diameter is measured at end-expiration, and collapsibility after sniff maneuver is calculated as IVCd-exp − IVCd-sniff/IVCd-exp, where IVCd-exp is IVCd at end-expiration and IVCd-sniff is IVCd after sniff maneuver. Respirometer tracing (*left arrow*) illustrates expiration (*bracket*) and sniff maneuver (*right arrow*). (C) M-mode image of inferior vena cava collapsibility index (cIVC) of 47.6% suggesting possible fluid responsiveness in a spontaneously breathing patient. The cIVC is calculated as IVCd-max − IVCd-min/IVCd-max, where IVCd-max is maximum IVCd (end-expiration, *left bracket*) and IVCd-min is minimum IVCd (inspiration, *right bracket*). (D) M-mode image of inferior vena cava distensibility index (dIVC) of 39.4% and IVCd variation index of 49.0%, both suggesting possible fluid responsiveness in a mechanically ventilated patient. dIVC is calculated as IVCd-max − IVCd-min/IVCd-min, where IVCd-max is maximum IVCd (end-inspiration, *right bracket* on respirometer) and IVCd-min is minimum IVCd (end-expiration, *left bracket* on respirometer). IVCd variation index is calculated as IVCd-max − IVCd-min/0.5(IVCd-max − IVCd-min).

Technique

Using TTE from a standard apical 4-chamber view, TAPSE is obtained by placing the M-mode line through the lateral tricuspid annulus (see Fig 5, A and B). The systolic excursion of the lateral tricuspid annulus is then measured from the lowest (end-diastole) to the highest (end-systole) points over an average of 3 heartbeats.[10]

With TEE, parallel alignment between the M-mode vector and direction of tricuspid annular motion can be challenging. However, the transgastric 4-chamber view has been shown to be feasible and reliable compared with TAPSE by TTE, even intraoperatively.[80,81] It is recommended to retroflex the TEE probe to increase parallel alignment of the M-mode vector and annular motion.

Clinical Implications

TAPSE is recommended as an overall index of RV function and prognostic factor in patients with pulmonary hypertension,[82-84] pulmonary embolism,[85,86] acute respiratory distress syndrome,[87] congestive heart failure,[88-90] and postcardiotomy shock,[91] all of which are commonly found in patients in the ICU. Furthermore, because LV function represents an important portion of RV function, there is close correlation between TAPSE and LV function; TAPSE <24 mm predicts higher in-hospital and long-term mortality rates and longer hospital stay.[92,93] The American Society of Echocardiography (ASE) established a cutoff value of <17 mm as an indicator of RV dysfunction (see Fig 5, B and C).[54,75]

Limitations

Similarly to MAPSE, TAPSE is angle dependent, may be preload dependent, and may not be valid in the presence of regional RV wall–motion abnormalities.[75] In patients with RV dilation and ensuing RV failure, TAPSE may be in the normal range because of some adaptation in the form of

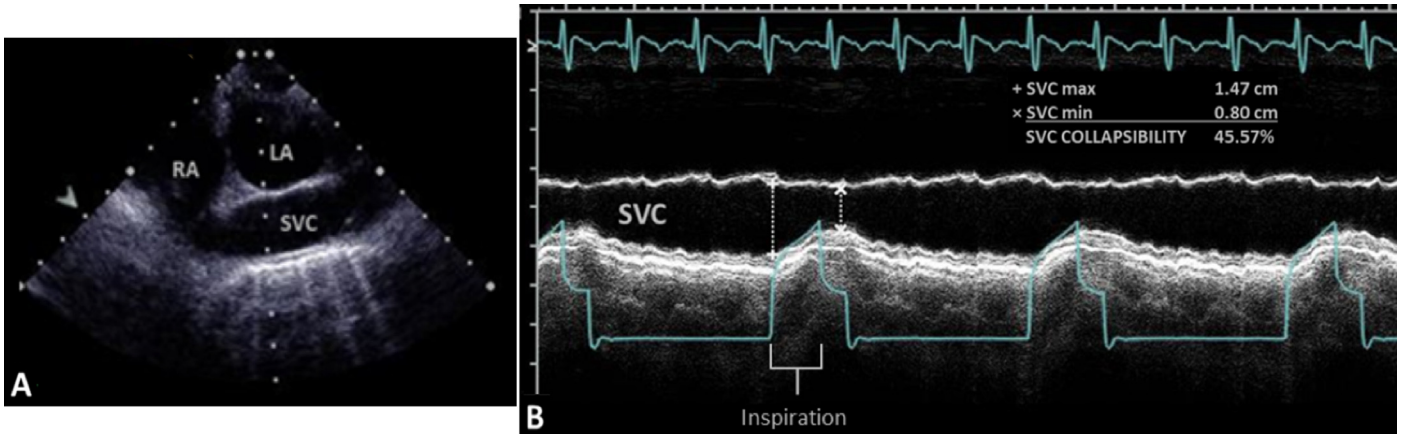

Fig 10. Superior vena cava assessment by transesophageal echocardiography. (A) Two-dimensional image of high esophageal view at the great vessels describing the image acquisition before M-mode imaging of the superior vena cava; the M-mode line (*middle white dotted line*) is placed through the left atrium and superior vena cava; then, M-mode imaging can be recorded. (B) M-mode image of superior vena cava collapsibility index (cSVC) of 45.5%, suggesting possible fluid responsiveness. The cSVC is calculated as SVC-max − SVC-min/SVC-max, where SVC-max is maximum superior vena cava diameter (end-expiration) and SVC-min is minimum superior vena cava diameter (end-inspiration, *bracket*). The respirometer tracing (*lower blue line*) illustrates the respiratory cycle. LA, left atrium; RA, right atrium; SVC, superior vena cava. Used with permission of Mayo Foundation for Medical Education and Research. All rights reserved.

increased contractility (Anrep mechanism), although it is insufficient.[94] Moreover, image acquisition of the apical 4-chamber TTE view in mechanically ventilated patients with limited mobility can be challenging.[95] In addition, because the TEE technique is characterized by suboptimal angling (nontangential) between the M-mode scan line and the tricuspid annular plane, TAPSE by TEE is frequently challenging. Finally, in patients with previous tricuspid valve annuloplasty, TAPSE underestimates RV function.[96]

Subcostal Echocardiographic Assessment of Tricuspid Annulus Kick

Given the aforementioned technical limitations of TAPSE image acquisition in patients in the ICU, an alternative measurement to TAPSE has been proposed—SEATAK.[95] Indeed, SEATAK, which is similar to TAPSE, evaluates RV function as RV longitudinal function but in the subcostal window.

Table 2
M-Mode Echocardiographic Parameters of Left Ventricular Function

Parameter	Echocardiographic Views	Clinical Correlation of Abnormal Values	Main Limitations
MAPSE	TTE: A4C TEE: HE4C	< 8 mm = LV systolic dysfunction; abnormal diastolic parameters (e′, E/e′); markers of myocardial injury in septic shock; worse outcomes in septic shock and Takotsubo cardiomyopathy	Unreliable in the presence of RWMA, mitral valve calcification, severe LV hypertrophy, atrial fibrillation, and at oldest and youngest ages (overestimates in young patients)
EPSS	TTE: PLAX	> 7 mm = severe LV systolic dysfunction Reliable in the presence of RWMA, except those on the anteroseptal wall	Unreliable in the presence of mitral stenosis, mitral valve calcification, aortic regurgitation, severe LV hypertrophy, and septal hypertrophy
LVFS	TTE: PLAX TEE: TGSAX	Endocardial: <27% for women, <25% for men; midwall: <15% for women, <14% for men = LV systolic dysfunction Particularly useful in LV concentric hypertrophy	Unreliable in the presence of RWMA, asymmetrically enlarged left ventricle
Vp	TTE: A4C TEE: ME4C	< 56 cm/s = LV diastolic dysfunction in patients with preserved LVEF Particularly useful with pseudonormal filling pattern	Unreliable in the presence of atrial fibrillation, HCM Complex image acquisition
Vp/Ap	TTE: A4C TEE: ME4C	< 1.06 = LV diastolic dysfunction in patients with preserved LVEF Particularly useful with pseudonormal filling pattern	
Vs	TTE: A4C TEE: ME4C	< 199 cm^2/s = reduced intraventricular pressure gradient (<2.2 mmHg); <155 cm^2/s = increased pulmonary capillary wedge pressure (>18 mmHg) Particularly useful in HCM	Unreliable in the presence of atrial fibrillation Complex image acquisition

Abbreviations: A4C, apical 4-chamber view; EPSS, E-point septal separation; HE4C, high-esophageal 4-chamber view; HCM, hypertrophic cardiomyopathy; LV, left ventricular; LVEF, left ventricular ejection fraction; LVFS, left ventricular fractional shortening; MAPSE, mitral annular plane systolic excursion; ME4C, midesophageal 4-chamber view; PLAX, parasternal long-axis view; RWMA, regional wall-motion abnormalities; TEE, transesophageal echocardiography; TGSAX, transgastric short-axis view; TTE, transthoracic echocardiography; Vp, early propagation velocity; Vp/Ap, early to late propagation velocity; Vs, product of Vp and distance to the deceleration point.

Technique

After obtaining a standard subcostal TTE window, the probe is rotated counterclockwise to create a subcostal IVC view, wherein the right atrium (RA), right ventricle, tricuspid annulus, and IVC are seen on the same image. The depth can be decreased to 14 to 18 cm to enhance image resolution. Then, the M-mode vector is placed through the lateral tricuspid annulus, which should be in the center of the sector width, and a linear measurement from end-diastole to end-systole (tricuspid annulus kick) is acquired (see Fig 6, A and B).

Clinical Implications

In a study of 45 critically ill patients, SEATAK, unlike TAPSE, was measured successfully in all patients.[95] Furthermore, SEATAK significantly correlated with TAPSE, especially in patients who had more severely decreased RV function.

Limitations

Similar to TAPSE, SEATAK appears to be preload dependent. Evidence is limited to 1 study evaluating SEATAK correlation with parameters of RV function.

Right Ventricular Outflow Tract Fractional Shortening

Because of the complex geometry of the right ventricle, comprehensive echocardiographic evaluation is challenging. However, the RVOT FS is a simple parameter that has shown substantial correlation with RV function.[97,98]

Technique

Using the parasternal short-axis view (TTE) at the level of the aortic root, the M-mode vector is placed through the RVOT wall centered in the sector width (see Fig 7, A) and, using endocardial cutting-edge methods, the percentage decrease in RVOT end-diastolic diameter that occurs by the end of systole is calculated, as follows:

$$\text{RVOT FS} = \text{RVOTDd} - \text{RVOTDs}/\text{RVOTDd} \times 100$$

where RVOTDd is the RVOT diameter at end-diastole and RVOTDs is the RVOT diameter at end-systole (see Fig 7, B).[97]

Clinical Implications

RVOT FS correlates with well-established RV dysfunction parameters such as TAPSE, tricuspid regurgitant velocity, and pulmonary artery acceleration time.[97] RVOT FS <32% identifies RV dysfunction with a sensitivity of 93% and specificity of 98% (see Fig 7, B and C).[98] When studied in patients with LV systolic dysfunction, RVOT FS was linked to LVEF, RV fractional area change, and brain natriuretic peptide value, thereby indicating its relationship to the performance of both the right and left ventricles.[99] Furthermore, in patients with acute pulmonary embolism, a lower RVOT FS was significantly associated with a higher pulmonary embolism severity index and a higher short-term mortality rate.[100] Lastly, an RVOT FS value <26% predicts low central venous pressure (≤8 mmHg) with a sensitivity of 95% and a specificity of 80%.[101]

Limitations

A subtle oblique direction of the M-mode vector at the RVOT may underestimate the measurement. Moreover, in patients with high central venous pressure, RVOT FS cannot be used to distinguish volume from pressure strain.

Ventricular Septum

Motion of the VS reflects the pressure gradient between the right and left ventricles. VS motion is, indeed, an integral component of LV performance, but certain pathologic conditions that affect the right ventricle, such as RV volume or pressure overload, affect VS motion; in these clinical scenarios, VS motion more closely reflects right-sided heart hemodynamics.[84]

Technique

With TTE, the parasternal short-axis view at the midpapillary level generally is used, but the parasternal long-axis view with the M-mode vector line placed across the RVOT and below the tips of the anterior mitral leaflet is considered the most sensitive (see Fig 8, A). With TEE, the transgastric short-axis view is recommended. Normal septal motion consists of thickening and concomitant inward movement toward the center of the left ventricle during systole (see Fig 8 B).[10,102]

Clinical Implications

RV volume overload, a condition caused by tricuspid or pulmonary regurgitation or atrial septal defect, results in a leftward shift and flattening of the VS, predominantly at mid-diastole and end-diastole, which creates a "D-shaped" LV appearance in early systole. During systole, the VS returns to its normal relative configuration, which results in an excessive rightward motion (paradoxical motion). In contrast, RV pressure overload, a disorder caused by pulmonary stenosis, pulmonary hypertension, or massive pulmonary embolism, results in a leftward shift and flattening of the VS throughout the entire cardiac cycle, with the most marked deformation at end-systole.[75,103] Overall, the leftward shift and flattening of the VS reduces LV filling regardless of preload conditions, thereby decreasing LV diastolic compliance. The ASE recommends evaluation of the VS throughout the cardiac cycle with 2D and M-mode TTE in conditions related to RV overload.[75]

In patients supported with mechanical ventilation, high positive end-expiratory pressure (PEEP) is well-known to cause LV dysfunction.[104] In patients with acute respiratory distress

syndrome, Jardin et al.[105] found that increased PEEP was associated with a leftward shift and flattening of the VS throughout the cardiac cycle, with a "D-shaped" LV appearance, a pattern similar to that observed in RV pressure overload. This finding suggested that the deleterious cardiovascular effects of PEEP were mainly mediated by ventricular interdependence, during which the right ventricle is limited by increased afterload (high PEEP) and LV performance is restrained. In addition, volume loading did not restore cardiac output and, in turn, increasingly accentuated the leftward shift of the VS, further impairing LV filling.

In patients with severe asthma, Jardin et al.[106] also described a leftward shift and flattening of the VS as a major contributor to the transitory decrease in LV cardiac output during inspiration (ie, pulsus paradoxus) (see Fig 8, C). This phenomenon accounts for exaggerated ventricular interdependence as a result of acute RV overload (induced by augmented systemic venous return and increased impedance to RV ejection) and lung distention that compresses the heart chambers.

In patients with chronic pulmonary hypertension, Mori et al.[107] characterized a pattern of abnormal septal motion that consists of an early systolic brisk rightward motion (toward the right ventricle) and a persistent posterior bulging (toward the left ventricle) throughout diastole. This motion was associated with worse clinical and hemodynamic status, including low cardiac index as an independent predictor. This abnormal septal motion is believed to reflect the progressive increase in RV diastolic pressures and mean right atrial pressure as a result of chronic pulmonary hypertension, thus leading to RV failure.

In severe RV dysfunction and pericardial constriction, VS bouncing is best seen on M-mode in the parasternal long-axis view (TTE); this parameter, when coupled with additional 2D and Doppler findings, can aid in the diagnosis of these conditions. In these cases, the relatively adynamic RV free wall is static while blood flows into the right ventricle, and as the right ventricle fills in diastole, the VS begins to shift toward the left ventricle. Then, in early systole, a more dynamic septal bounce toward the left ventricle occurs.

In some patients with LBBB, a brief leftward dip, or "beak," of the VS (toward the left ventricle) can be recognized shortly after the onset of electrical depolarization, followed by rightward (paradoxical) motion (toward the right ventricle) of the VS, that persists throughout systole.[108] This leftward septal dip is caused by the abnormal depolarization of the VS inherent to LBBB physiology. The paradoxical septal motion in LBBB is considered equivalent to an akinetic or dyskinetic VS due to myocardial infarction (lower cardiac performance). LBBB can also present with a brief leftward septal dip that is followed by normal leftward motion rather than rightward septal motion during systole (abnormal); this is called benign, or nonparadoxical, LBBB.[13]

Limitations

Analysis of septal motion for RV overload conditions is not reliable in the presence of conduction delays, particularly LBBB. Moreover, in postcardiac surgery patients, septal motion abnormalities, although common, are not correlated to LV or RV function; they appear to be caused by excessive forward cardiac motion from fixation of the heart anteriorly by postoperative sternal-cardiac adhesions.[109,110]

Right Ventricular Afterload Changes

Right Ventricular Wall Thickness

Right ventricular wall thickness (RVWT) is a useful parameter for the diagnosis of RV hypertrophy, which usually is the result of RV systolic pressure overload over time (chronicity), although it also is seen in patients with substantial LV hypertrophy, including HCM.[112,113]

Technique

With TTE, the subcostal 4-chamber or parasternal long-axis view is preferred. With TEE, the transgastric short-axis view can be used. The M-mode vector should be aligned perpendicular to the RV free wall, and the RVWT should be measured at end-diastole while carefully excluding trabeculations, papillary muscle, and epicardial fat. The ASE provides a cutoff value of >5 mm for RV hypertrophy.[10,75,113]

Clinical Implications

In patients with chronic RV overload, RV hypertrophy measured by M-mode TTE predicts increased RV systolic pressures; RV wall thickness >4 mm predicts pulmonary hypertension with excellent sensitivity (97%) and specificity (90%) in this patient population, although it is not uncommon for these patients to have an RVWT ≥ 10 mm.[114] In contrast, in a single study, patients with acute RV overload (acute respiratory distress syndrome, acute cor pulmonale) were observed to develop an acute, reversible increase in RVWT after 48 hours of positive pressure ventilation, up to an average of 6.5 mm.[113] Such a phenomenon supports the concept that regional changes in RV structure and function may be early markers of the risk of severe RV dysfunction.[115] In another study, RV hypertrophy documented by M-mode TTE in patients with HCM was significantly associated with more severe disease features (severe LV hypertrophy, supraventricular arrhythmias, and ventricular tachycardia).[116]

Limitations

In the presence of thickened visceral pericardium, measurement of the RVWT may be challenging. A careful evaluation of the RV free wall in the subcostal and parasternal long-axis view should be considered complementary for final thickness grading.

Right Ventricular Outflow Tract Obstruction

RVOT obstruction (RVOTO), defined as a peak RV-to-pulmonary artery systolic gradient >25 mmHg, is a source of hemodynamic derangement within surgical populations that

may arise either from a fixed or dynamic obstruction.[117] The reported incidence of RVOTO in the cardiac surgical population ranges from 1% to 4%.[117] Risk factors for the development of RVOTO include anatomic hypertrophy and an acute decrease in physiological afterload.[118]

Technique

With TEE, the RVOT view may be obtained from the midesophageal RV inflow-outflow view, with the M-mode vector placed through the area of narrowing proximal to the pulmonary valve. Advancement of the omniplane, with rotation of the probe slightly to the right, will avoid foreshortening, and generally the entire RVOT can be observed just proximal to the pulmonary valve.[119] The diagnosis of obstruction is confirmed with end-systolic obliteration of the RVOT cavity, which may be accompanied by systolic fluttering of the pulmonary valve, which may be seen on both M-mode and color Doppler modalities.[117,120] In TTE, the parasternal short-axis view can be used to view the RVOT, with a similar approach to the RVOT FS previously described.[119]

Clinical Implications

Physical compression from mediastinal structures, hematoma, or surgical manipulation can result in extrinsic RVOTO, whereas acute decreases in afterload or preload or increases in contractility can result in intrinsic RVOTO. The resultant hemodynamic instability from RVOTO can be dynamic with changing physiological parameters or can be fixed with relatively static anatomic restrictions.[117] Populations reported to be at risk for RVOTO include patients postcardiopulmonary bypass, patients with HCM, or lung transplantation recipients.[117-119,121] Of note, the lung transplantation population, because of both chronic RV remodeling and a decrease in RV afterload associated with new graft implantation, is at risk for acute or delayed RVOTO, even months after transplantation.[118,121]

Limitations

Foreshortening of the RVOT in either the TTE or TEE image planes can result in a false diagnosis of end-systolic obliteration using M-mode. Extrinsic compression due to anatomic structures or hematoma may result in echocardiographic artifacts limiting the view of the RVOT in TTE windows. The quality of parasternal short-axis windows also may be limited perioperatively in lung transplantation patients who underwent a clamshell surgical approach. Table 3 provides a summary of the M-mode echocardiographic parameters of RV function.

Volume Status and Responsiveness

Inferior Vena Cava in Spontaneously Breathing Patients

The IVC is a compliant blood vessel; its caliber is altered by intravascular volume status, right-sided heart function, and respiration.[122,123] In normovolemic, spontaneously breathing patients, inspiration (or a brief sniff) causes negative intrathoracic pressure, which in turn increases venous return to the right side of the heart and consequently decreases (or collapses) the IVC lumen diameter. In hypovolemic, spontaneously breathing patients, the IVC collapse is exaggerated.

Technique

After a standard subcostal TTE view is obtained, the RA is placed in the middle of the sector width, and the probe is rotated counterclockwise until the probe marker is pointing cephalad (12-o'clock position); the IVC should be seen on its longitudinal axis, the junction between the IVC and RA must be kept on the screen, and the M-mode line should be placed perpendicularly and across the IVC at 2 to 3 cm before its entry to the RA (see Fig 9, A).[3] The IVC diameter (IVCd) is measured at end-expiration. The IVC collapsibility index (cIVC) is calculated as follows:

$$\text{cIVC} = \text{IVCd}-\text{max} - \text{IVCd}-\text{min}/\text{IVCd}-\text{max} \times 100$$

where IVCd-max is the maximum IVCd (end-expiration) and IVCd-min is the minimum IVCd (inspiration) (see Fig 9, C).[54]

Clinical Implications

In spontaneously breathing patients, IVC measurements accurately predict right atrial pressure (RAP),[124] which allows for prompt identification of extremely hypovolemic patients and facilitates the echocardiographic calculation of right-sided heart pressures (RV and pulmonary artery systolic pressures).[75,125] The ASE has established the following cutoff values: IVCd <2.1 cm that collapses >50% with a sniff suggests a RAP of 3 mmHg (0-5 mmHg) (see Fig 9, B); IVCd >2.1 cm that collapses <50% with a sniff suggests a RAP of 15 mmHg (10-20 mmHg). If the IVC diameter and percentage collapse do not fit this paradigm, a value of 8 mmHg (5-10 mmHg) is recommended as the estimated RAP.[54,126] Lastly, in patients who are unable to adequately perform a sniff, an IVC that collapses <20% with quiet inspiration suggests high RAP.[75]

Fluid responsiveness is universally defined as an increase in cardiac index or cardiac output of ≥15% after intravascular volume expansion (ie, fluid challenge).[122,127] In the past decade, several studies have evaluated the utility of cIVC as a predictor of fluid responsiveness and as a guide for fluid management in spontaneously breathing, critically ill patients with acute circulatory failure.[127-131] Three studies—those of Muller et al.,[130] Preau et al.,[131] and Airapetian et al.[129]—found that under spontaneous breathing, cIVC values of 40%, 41%, and 42% or more, respectively, could predict fluid responsiveness with good specificity but poor sensitivity (see Fig 9, C). Moreover, Preau et al.[131] included only patients with septic shock and compared the cIVC after a standardized versus spontaneous breathing technique. With a standardized breathing technique, a cIVC ≥48% predicted fluid responsiveness with a sensitivity of 84% and specificity of 90%. In another small study of 14 patients with septic shock, Lanspa et al.[127] found that a cIVC cutoff value of 15% could exclude fluid responsiveness (negative predictive value of 100%). However, the patient populations in these studies were

Table 3
M-Mode Echocardiographic Parameters of Right Ventricular Function

Parameter	Echocardiographic Views	Clinical Correlation of Abnormal Values	Main Limitations
TAPSE	TTE: A4C TEE: TG4C	<17 mm = RV dysfunction and prognostic factor in pulmonary hypertension, pulmonary embolism, ARDS, congestive heart failure, postcardiotomy shock	Unreliable in the presence of RWMA, prior tricuspid valve annuloplasty, and RV dilation Challenging image acquisition in ICU patients
SEATAK	TTE: SC	Significantly correlated with TAPSE Easy image acquisition	Novel parameter, yet to be validated
RVOT FS	TTE: PSAX-AV	<32% = RV dysfunction; worse outcomes in pulmonary embolism	Unreliable in patients with high central venous pressure
Ventricular septum A: Leftward shift (bowing) or flattening B: Paradoxical septal motion	TTE: PLAX, PSAX-MP TEE: TGSAX	RV volume overload: A, During diastole (sparing of LV deformation at end of systole) RV pressure overload: A, At end-systole/early diastole Constrictive pericarditis: A, at early diastole (important for distinguishing from restrictive cardiomyopathy) Left bundle branch block, anteroseptal infarction, postcardiotomy (transient): B, During systole Arrhythmogenic RV cardiomyopathy: B, During diastole	Lack of predictability of septal wall motion abnormality and the degree of RV dysfunction
RVWT	TTE: SC TEE: TGSAX	>5 mm = RV hypertrophy; worse outcomes in HCM >4 mm, in chronic RV overload = pulmonary hypertension	Challenging image acquisition in the presence of thickened visceral pericardium Slight thickening (5-6 mm) has been described in acute cor pulmonale (ie, ARDS)
RVOTO	TTE: PSAX TEE: MEIO	Extrinsic compression (eg, mediastinal structures, hematoma, surgical manipulation); intrinsic compression (eg, acute decreases in afterload or preload, increases in contractility) Particularly useful after cardiotomy bypass, HCM, lung transplantation	Challenging image acquisition, especially in extrinsic compression and lung transplantation

Abbreviations: A4C, apical 4-chamber view; ARDS, acute respiratory distress syndrome; HCM, hypertrophic cardiomyopathy; ICU, intensive care unit; LV, left ventricular; MEIO, midesophageal right ventricular inflow-outflow view; PLAX, parasternal long-axis view; PSAX-AV, parasternal short-axis view, aortic valve level; PSAX-MP, parasternal short-axis view, midpapillary level; RV, right ventricular; RVOTO, right ventricular outflow tract obstruction; RVOT FS, right ventricular outflow tract fractional shortening; RVWT, right ventricular wall thickness; RWMA, regional wall-motion abnormalities; SC, subcostal view; SEATAK, subcostal echocardiographic assessment of tricuspid annulus kick; TAPSE, tricuspid annular plane systolic excursion; TEE, transesophageal echocardiography; TG4C, transgastric 4-chamber view; TGSAX, transgastric short-axis view; TTE, transthoracic echocardiography.

small and considerably homogenous. Overall, it appears that either very large or very small values of cIVC may have some utility in reliably predicting or excluding fluid responsiveness in patients with acute circulatory failure, particularly that due to sepsis. The cIVC therefore should be interpreted cautiously and be used as a complementary tool and not as a single parameter to guide fluid therapy. Many ultrasound protocols for critically ill patients have, nonetheless, included cIVC assessment as an important parameter.[132-134]

Among spontaneously breathing patients undergoing elective noncardiac surgery, intravascular fluid therapy guided by cIVC before spinal anesthesia was found to be an effective method to prevent postspinal anesthesia hypotension.[135]

Limitations

Spontaneous breathing implies complex and variable physiological and hemodynamic effects that place a natural limit on the use of a dynamic parameter, as follows: (1) translation movement of the IVC due to respiration mechanics prevents measuring the IVCd at the same point at different times throughout a respiratory cycle[136]; (2) spontaneously breathing patients who are critically ill, especially those with dyspnea, have a wide range of breathing patterns, which causes inconsistent tidal volumes and intrathoracic pressures in a given patient and among different patients; and (3) IVCd is affected by diaphragmatic motion, which varies substantially according to the strength of inspiratory effort at the moment of measurement. A recent study[137] found that high inspiratory effort predicted a cIVC >40%.

Furthermore, there is no consensus on the exact anatomic location for the IVC measurements, and therefore different locations have been used across studies. Wallace et al.[138] demonstrated that measurements taken at the junction of the RA and IVC are not equivalent to those at other sites. Also, in healthy young athletes, the IVC may be dilated in the presence of normal RAP.[139] Moreover, IVC measurements may not be

feasible in the operating room, and in patients on mechanical ventilators, IVC measurements do not correlate with RAP; however, in this same patient population, an IVC diameter ≤1.2 cm accurately predicted RAP <10 mmHg, and a small and collapsed IVC suggested hypovolemia.[75]

Inferior Vena Cava in Mechanically Ventilated Patients

In contrast to spontaneously breathing patients, patients receiving mechanical ventilator support have positive intrathoracic pressure during inspiration, which in turn decreases venous return to the right-sided heart chambers and consequently increases (or distends) the IVC lumen diameter. This distention is assumed to reflect a preload reserve; the higher the distention, the higher the preload reserve.

Technique

Although mainly measured by TTE with the technique previously described, IVCd and respiratory variation as measured by TEE also are reliable and particularly useful in anesthetized, mechanically ventilated patients; this can be achieved from a standard bicaval long-axis view.[140] For reproducibility purposes, the studies cited in the following investigated ventilated patients without spontaneous breathing efforts and with the following standard ventilator settings when measuring IVCd: tidal volume of 7 to 8 mL/kg, PEEP of 4 to 6 cmH_2O, and breathing rate of 15 to 18 respirations/min.

Clinical Implications

Two studies—those of Barbier et al.[122] and Feissel et al.[141]—investigated respiratory variation in IVCd to predict fluid responsiveness in mechanically ventilated patients with acute circulatory failure due to sepsis. Barbier et al.[122] studied the IVC distensibility index (dIVC), which is calculated as follows:

$$\text{dIVC} = \text{IVCd}-\text{max}-\text{IVCd}-\text{min}/\text{IVCd}-\text{min}$$

where IVCd-max is maximum IVCd (end-inspration) and IVCd-min is minimum IVCd (end-expiration). They showed that a cutoff value of 18% predicted volume responsiveness with a sensitivity of 90% and specificity of 90%. In contrast, Feissel et al.[141] evaluated the IVCd variation index, which is calculated as follows:

$$\text{IVCd variation index} = \text{IVCd}-\text{max}-\text{IVCd} -\text{min}/0.5(\text{IVCd}-\text{max}+\text{IVCd}-\text{min}) \times 100$$

They found that a cutoff value of 12% predicted volume responsiveness with positive and negative predictive values of 93% and 92%, respectively. Furthermore, both studies found a strong correlation between IVCd respiratory variation and cardiac output increase after volume expansion (ie, the higher the IVCd respiratory variation before volume expansion, the greater the increase in cardiac output in response to volume expansion) (see Fig 9, D). Later, a dIVC value of >16% was found to be a reliable predictor of fluid responsiveness in mechanically ventilated patients with subarachnoid hemorrhage.[142] These studies, however, were done in small, homogenous series of patients. In a recent multicenter study conducted among 540 unselected patients with acute circulatory collapse of any cause, dIVC had moderate accuracy and low sensitivity to predict fluid responsiveness.[143] Overall, the usefulness of IVC respiratory variation to predict fluid responsiveness in mechanically ventilated patients appears to have considerable clinical relevance but requires confirmatory studies.[144]

Compared with IVCd respiratory variability, the end-expiratory IVCd is expected to be a more feasible and reproducible parameter that is less dependent on operator skills and ventilator settings.[144,145] In an ancillary study[146] by Vignon et al.,[143] end-expiratory IVCd was moderately feasible (unable to obtain in 22% of patients) and was substantially modified by high intra-abdominal pressure (confounding factor), which was present in 30% of patients. End-expiratory IVCd poorly predicted fluid responsiveness, with a specificity of 80% for cutoff values of ≤13 mm for responders and ≥25 mm for nonresponders, although 70% of the patients had values between these cutoffs. Similarly, in a small cohort of 39 ventilated patients with septic shock, all patients who were fluid responders had an end-expiratory IVCd ≤10 mm.[141] Thus, extreme values of end-expiratory IVCd might add some value to guide fluid therapy but should not be used alone to predict fluid responsiveness.

Limitations

The points discussed in the previous section (IVC in Spontaneously Breathing Patients) also should be taken into account here. Furthermore, IVC measures do not estimate fluid responsiveness when mechanical ventilation is performed with assisted modalities (eg, pressure support ventilation) or in the presence of high intra-abdominal pressures (abdominal compartment syndrome).[145,146] It also is probable that the infusion of vasopressors, which is not uncommon in patients with mechanical ventilation, can alter IVCd respiratory variation.[122]

Superior Vena Cava in Mechanically Ventilated Patients

In mechanically ventilated patients, the SVC, which has an entirely intrathoracic location, collapses during inspiration; the degree of SVC collapse has been closely correlated to intravascular volume status.[147]

Technique

With TEE, the SVC is easily visualized using the high-esophageal view at the great vessels; M-mode–derived measures of SVC diameter (SVCd) and respiratory variation are obtained by placing the M-mode vector 1 to 2 cm away from the SVC entry point into the RA (see Fig 10, A). The SVC collapsibility index (cSVC) is calculated from a long-axis view of the SVC (rotating

the ultrasound beam by 90 degrees), as follows:

$$cSVC = SVCd-max - SVCd-min / SVCd-max \times 100$$

where SVCd-max is maximum SVCd (end-expiration) and SVCd-min is minimum SVCd (end-inspiration) (see Fig 10, B).

Clinical Implications

In mechanically ventilated patients with acute circulatory failure, the cSVC has been proven to be a reliable predictor of fluid responsiveness. In a series of 66 patients with septic shock, Vieillard-Baron et al.[148] showed that a cSVC cutoff of 36% predicts fluid responsiveness with a sensitivity of 90% and a specificity of 100%. In a recent multicenter study[143] including 540 mechanically ventilated patients with various causes of circulatory shock, the cSVC had the best feasibility, specificity, and diagnostic accuracy compared with pulse pressure and IVCd respiratory variations, although its accuracy was much lower than that reported in the previous study.

Limitations

SVC cannot be properly evaluated by TTE and thus strictly requires TEE. Also, unlike IVCd and IVC collapse after sniff maneuver, SVCd and cSVC do not reliably reflect RAP, which is useful for RV pressure and pulmonary arterial pressure estimates.[143,149] Table 4 provides a summary of the M-mode echocardiographic parameters of volume status and responsiveness.

Table 4
M-Mode Echocardiographic Parameters of Volume Status and Responsiveness Assessments

Parameter	Echocardiographic Views	Clinical Correlation of Abnormal Values	Main Limitations
End-expiratory IVC diameter and sniff collapsibility	TTE: SC	Diameter <2.1 cm, collapses >50% during sniff = RAP 0-5 mmHg (3 mmHg) Diameter >2.1 cm, collapses <50% during sniff = RAP 10-20 mmHg (15 mmHg) Diameter <2.1 cm, collapses <50% during sniff or diameter >2.1 cm, collapses >50% = RAP 5-10 mmHg (8 mmHg)	In healthy young athletes, IVC may be dilated in the presence of normal RAP
End-expiratory IVC diameter	TTE: SC	Diameter ≤13 mm and ≥25 mm after standard mechanical ventilation may predict fluid responsiveness and unresponsiveness, respectively	Moderately feasible Very low sensitivity and low positive predictive value Unreliable in the presence of high intra-abdominal pressures (abdominal compartment syndrome)
IVC collapsibility index	TTE: SC	>40%-42% after spontaneous breathing technique may predict fluid responsiveness in acute circulatory failure, especially septic shock ≥48% after standardized breathing technique may predict fluid responsiveness in septic shock	Poor reproducibility because of extreme variability in exact anatomic location for IVC measurement, IVC translation movement, spontaneous breathing pattern and technique, and diaphragmatic motion among patients
IVC distensibility index	TTE: SC	>18% after standard mechanical ventilation may predict fluid responsiveness in septic shock	Poor reproducibility because of extreme variability in exact anatomic location for IVC measurement and IVC translation movement Unreliable in the presence of high intra-abdominal pressures (abdominal compartment syndrome), vasopressor agents, and assisted mechanical ventilation modalities (pressure support ventilation)
IVC diameter variation index	TTE: SC	>12% after standard mechanical ventilation may predict fluid responsiveness in septic shock	Poor reproducibility because of extreme variability in extact anatomic location for IVC measurement and IVC translation movement. Unreliable in the presence of high intra-abdominal pressures (abdominal compartment syndrome), vasopressor agents, and assisted mechanical ventilation modalities (pressure support ventilation)
SVC collapsibility index	TEE: HE	>36% after standard mechanical ventilation may predict fluid responsiveness in septic shock Optimized cutoff values: 4%, high sensitivity; 31%, high specificity	Unreliable for RAP estimates

Abbreviations: HE, high-esophageal view; IVC, inferior vena cava; RAP, right atrial pressure; SC, subcostal view; SVC, superior vena cava; TEE, transesophageal echocardiography; TTE, transthoracic echocardiography.

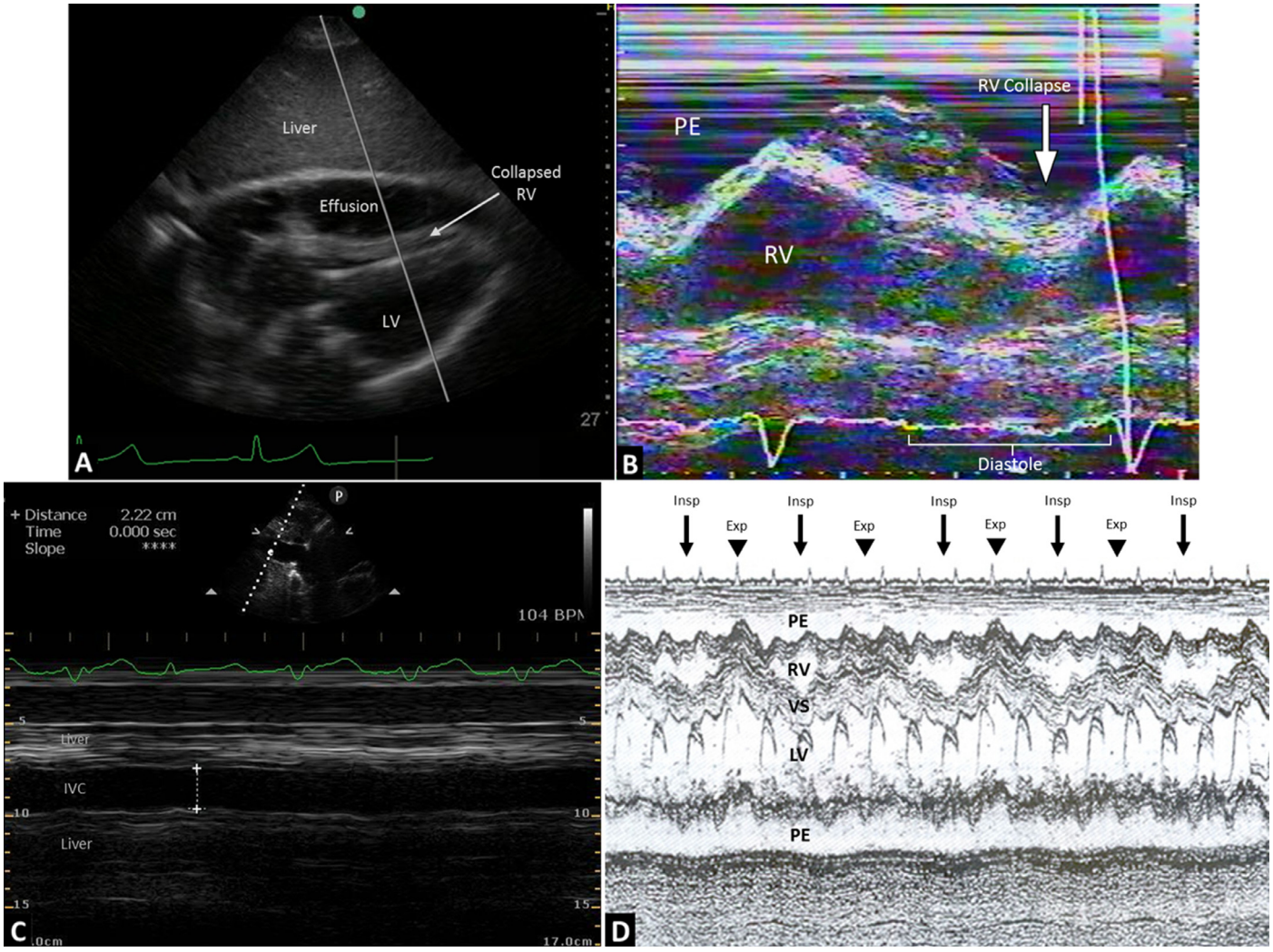

Fig 11. Cardiac tamponade assessment by transthoracic echocardiography. (A) Two-dimensional image of subcostal window, 4-chamber view describing the image acquisition before M-mode imaging of right ventricular free wall inversion in a patient with cardiac tamponade; the M-mode line (*gray line*) is placed through the collapsed right ventricle, ventricular septum, and left ventricle; then, M-mode imaging can be recorded. (B) M-mode image of right ventricular free wall inversion (*arrow*) during diastole (*bracket* below electrocardiographic tracing) in a patient with cardiac tamponade. (C) M-mode image of inferior vena cava plethora in a patient with cardiac tamponade (ie, large inferior vena cava diameter without respiratory variation). (D) M-mode image of respiratory variation in ventricular septal motion in a patient with large pericardial effusion and cardiac tamponade. During inspiration (*arrows*) there is leftward shift (toward the left ventricle) of the ventricular septum, whereas during expiration (*arrowheads*) there is normal motion of the ventricular septum. LV, left ventricle; PE, pericardial effusion; RV, right ventricle; VS, ventricular septum.

Specific Applications

Cardiac Tamponade

The most important first step in the management of pericardial effusion is to determine the presence of tamponade physiology and the potential need for urgent pericardiocentesis.[150] The most reliable echocardiographic indicators of impending tamponade are: (1) early diastolic RV free-wall inversion[151] (see Fig 11, A and B), (2) dilated IVC with absent respiratory variation (IVC plethora)[126] (see Fig 11, C), and (3) exaggerated respiratory variation in peak mitral (>30%) and tricuspid (>60%) blood flow velocities.[152] Two of these 3 indicators use M-mode imaging.

Technique

Because RV inversion or collapse has been found to be most prominent in the RVOT,[151] this parameter usually is evaluated using the parasternal long-axis view (TTE), with the M-mode vector placed perpendicular through the RV free wall, although the parasternal short-axis or subcostal views also can be used.

Clinical implications

Although RV collapse can be evident using 2D TTE, M-mode recording helps to identify, with more accuracy, subtle

chamber collapse and to confirm it is truly in diastole, particularly early diastole (at the end of the T wave on the electrocardiogram), when the RV intracavitary pressure is lowest and therefore is exceeded by the intrapericardial pressure.[13,151] In the presence of large pericardial effusion, a pattern of cardiac motion including 2 or more cardiac cycles can be identified on M-mode imaging; this alternating motion affects the electrocardiogram, causing the classic pattern of electrical alternans.[153] Furthermore, M-mode also permits observation of ventricular interdependence along the respiratory cycle. During inspiration, the RV dilates because of increased systemic venous return, RV diastolic collapse ceases, and the VS shifts leftward, which consequently restrains LV performance (see Fig 11, D). During expiration, the opposite is observed (conventional diastolic RV collapse and normal VS and LV configuration).[154] Tamponade physiology also causes retrograde congestion along the IVC.[155] The IVC therefore dilates (diameter >2.1 cm) and does not change throughout the respiratory cycle (see Fig 11, C). However, IVC dilation obviously is not specific to this situation.

Cardiac tamponade is nonetheless a clinical diagnosis that commonly requires echocardiography solely for identifying the pericardial effusion. In any case, the aforementioned parameters are useful to monitor response to intervention and the hemodynamic effect of effusion reaccumulation.[155]

Limitations

In patients with constrictive pericardial disease, tamponade may not cause diastolic RV collapse.[152] In the very rare situation in which cardiac tamponade is associated with profound hypovolemia (eg, trauma patients), the IVC may dilate only after fluid expansion.

Left Ventricular Outflow Tract Obstruction

Although dynamic LVOTO due to SAM of the mitral valve initially was linked only with HCM, it is now known to be associated with various conditions, including abnormal mitral valve apparatus, complicated aortic or mitral valve repair,[156] subaortic stenosis, hypertensive LV hypertrophy, myocardial infarction, general anesthesia,[157] and in patients with structurally normal hearts with septic shock[158] or on catecholamine therapy.[81,159-162] In general, SAM occurs in hypovolemic and hypercontractile states. The onset and duration of mitral leaflet-septal approach, which is used to grade SAM, are best depicted by M-mode imaging on TTE or TEE.[163,164]

Technique

With TTE, the parasternal long-axis view is used; with TEE, the midesophageal long-axis view is used. The M-mode vector must be placed through the anterior leaflet of the mitral valve. The electrocardiogram tracing is needed to correlate the M-mode imaging with the cardiac cycle.

Clinical Implications

Although septal hypertrophy, which can be measured with M-mode imaging, may also contribute to dynamic obstruction of the LVOT in patients with HCM, SAM of the mitral valve definitively has the primary role, which makes the M-mode–derived measurement of SAM a high-yield tool.[165] Moreover, demonstration of early aortic valve closure using M-mode imaging, and the same view for SAM, is a helpful finding that supports the diagnosis of SAM and consequent LVOTO.[81] The ASE recommends echocardiography as the imaging modality of choice for screening, diagnosis, monitoring, and therapy guidance in patients with HCM.[111]

In the ICU or operating room, hypotensive patients may be receiving inotropic therapy with or without vasopressors; however, if the patient is relatively hypovolemic and also has conditions associated with SAM, catecholamine therapy may result in LVOTO and consequent paradoxical hemodynamic deterioration.[156,161,162] Furthermore, SAM as a cause of perioperative hypotension usually develops in low-preload states, which may result from absolute hypovolemia (volume depletion) or relative hypovolemia (secondary to the vasodilatory effects of anesthetic agents or anaphylaxis).[166] Thus, LVOTO due to SAM can be easily unrecognized as the cause of hypotension or refractory shock, which may result in an erroneous treatment regimen that further deteriorates the hemodynamic status of the patient.[161] M-mode TTE or TEE, which is the simplest method for detecting SAM, provides feasible screening and early detection of this condition.

Limitations

In patients with HCM, appropriate echocardiographic assessment of dynamic LVOTO requires, in addition to M-mode TTE, pulsed- and continuous-wave Doppler measurements for detailed localization of the site of obstruction and determination of the peak gradient.[167]

Aortic Dissection

Although TEE is considered the diagnostic standard evaluation tool for aortic dissection, both TEE and TTE are recommended by the ASE.[168,169] The utility of M-mode imaging in the diagnosis of aortic dissection was described long ago and proved useful and feasible[170,171]; however, its current application is rather limited.

Technique

In both TEE and TTE, M-mode imaging is particularly useful for identifying the intimal flap, distinguishing the true lumen from the false lumen, and identifying artifacts, which are fundamental steps in the diagnosis of aortic dissection. In early systole, the pressure in the true lumen increases, expanding the true lumen and compressing the false lumen; M-mode imaging allows for accurate visualization and temporal correlation with

Table 5
M-Mode Echocardiographic Parameters of Specific Pathologic Conditions

Pathologic Process	Echocardiographic Views	Clinical Correlation of Abnormal Values	Main Limitations
Cardiac tamponade	TTE: PLAX, PSAX, SC	RV collapse at early diastole Leftward shift and flattening of ventricular septum during inspiration IVC plethora (IVC diameter >2.1 cm with absent respiratory variability)	Unreliable in constrictive pericardial disease, profound hypovolemia, positive-pressure mechanical ventilation, and status asthmaticus
LVOTO	TTE: PLAX TEE: MELAX	Systolic anterior motion of the mitral valve	Confirmation of LVOTO requires additional Doppler parameters
Aortic dissection	TTE: PLAX TEE: HE	Identification of the intimal flap, true lumen, false lumen, artifacts	Affected by aortic root aneurysm or abscess, mobile atherosclerotic plaque, dilated or calcified aortas, tumor, or superimposed vessels

Abbreviations: HE, high-esophageal view; IVC, inferior vena cava; LV, left ventricular; LVOTO, left ventricular outflow tract obstruction; MELAX, midesophageal long-axis view; PLAX, parasternal long-axis view; PSAX, parasternal short-axis view; RV, right ventricular; SC, subcostal view; TEE, transesophageal echocardiography; TTE, transthoracic echocardiography.

the cardiac cycle of the expansion of the true lumen and the related motion (or fluttering) of the intimal flap.[172,173]

Clinical Implications

Aortic dissection can present intraoperatively as sudden hemodynamic instability or hypoxia; in this scenario, rescue intraoperative TEE is a valuable tool that accurately identifies the intimal flap and tear entry, distinguishes the true from the false lumen, detects involvement of coronary artery ostia, and evaluates the presence and degree of aortic insufficiency and pericardial effusion.[174,175] Furthermore, artifacts found in TEE imaging of the ascending aorta may be interpreted as intimal flap (false-positive); however, unlike artifacts, intimal flap motion, which is best visualized by M-mode imaging, is unrelated to that of the aortic wall and instead is related to the cardiac cycle.[171,176] In this way, M-mode–derived information improves the sensitivity, specificity, and positive predictive value of TEE for the diagnosis of aortic dissection.[171] Moreover, when the intimal flap is located on the aortic arch, TEE may not identify it correctly; this phenomenon is known as the "blind spot." In this scenario, TTE complements TEE by providing a better assessment of the artic arch.[177]

In the only large study evaluating M-mode TTE measurements for the diagnosis of aortic dissection, by D'Cruz et al.,[178] the combination of M-mode and 2D TTE imaging proved to be a reliable and sensitive (88%) combination for the diagnosis of ascending aortic aneurysm, although much less for the diagnosis of descending thoracic aortic aneurysm. Interestingly, in this patient population, because of the potential impingement of a dilated ascending aorta on the chest wall to the right of the sternum, a right parasternal window (ie, the ultrasound probe placed over the second or third right intercostal space and perpendicular to the chest wall) provided better visualization of the ascending aorta than did the conventional left parasternal window.

Limitations

False-positive images of intimal flaps have been reported in patients with aortic root aneurysm or abscess, mobile atherosclerotic plaque, dilated or calcified aortas, tumor, or superimposed vessels, especially prominent valves within large innominate veins.[179,180] Table 5 provides a summary of the M-mode echocardiographic parameters of cardiac tamponade, LVOTO, and aortic dissection.

Conclusion

Resurgence of M-mode ultrasonography for newer applications in anesthesia and critical care settings appears reasonable. The increasing availability of multiple complementary monitoring systems is a hallmark of the contemporary perioperative medical practice. Indeed, echocardiography performed by noncardiologist physicians has enhanced inquisitiveness and has introduced many measurements that, although accurate, do not necessarily fit into an extremely dynamic scope of practice. M-mode echocardiography meets the pragmatism demanded by the contemporary anesthesiology and critical care medicine practice because it provides reliable, clinically relevant information that also is widely available and easily and quickly obtained. M-mode has the best temporal resolution among ultrasound modalities, is available with most basic ultrasound machines, requires standard sonographic views and single linear measurements, is interpreted based on simple pattern recognition, and is supported by a considerable body of literature.

Acknowledgment

The authors express their gratitude to Alyssa Biorn Quiggle, PhD, for her excellent medical editing skills.

References

1 Edler I, Lindstrom K. The history of echocardiography. Ultrasound Med Biol 2004;30:1565–644.
2 Moore CL, Copel JA. Point-of-care ultrasonography. N Engl J Med 2011;364:749–57.
3 Diaz-Gomez JL, Via G, Ramakrishna H. Focused cardiac and lung ultrasonography: Implications and applicability in the perioperative period. Romanian J Anaesth Intensive Care 2016;23:41–54.

4 Vieillard-Baron A, Slama M, Cholley B, et al. Echocardiography in the intensive care unit: From evolution to revolution? Intensive Care Med 2008;34:243–9.
5 International consensus statement on training standards for advanced critical care echocardiography. Intensive Care Med 2014;40:654–66.
6 Ryan T, Armstrong WF, Khandheria BK. Task force 4: Training in echocardiography: Endorsed by the American Society of Echocardiography. J Am Coll Cardiol 2008;51:361–7.
7 Mizubuti GB, Allard RV, Tanzola RC, et al. Pro: Focused cardiac ultrasound should be an integral component of anesthesiology residency training. J Cardiothorac Vasc Anesth 2015;29:1081–5.
8 Diaz-Gomez JL, Perez-Protto S, Hargrave J, et al. Impact of a focused transthoracic echocardiography training course for rescue applications among anesthesiology and critical care medicine practitioners: A prospective study. J Cardiothorac Vasc Anesth 2015;29:576–81.
9 Tanzola RC, Walsh S, Hopman WM, et al. Brief report: Focused transthoracic echocardiography training in a cohort of Canadian anesthesiology residents: A pilot study. Can J Anaesth 2013;60:32–7.
10 Otto C. Textbook of clinical echocardiography. ed 5 Philadelphia, PA: Elsevier/Saunders; 2013.
11 Edler I, Hertz CH. The use of ultrasonic reflectoscope for the continuous recording of the movements of heart walls. 1954. Clin Physiol Functional Imaging 2004;24:118–36.
12 Singh S, Goyal A. The origin of echocardiography: A tribute to Inge Edler. Texas Heart Institute J 2007;34:431–8.
13 Feigenbaum H. Role of M-mode technique in today's echocardiography. J Am Soc Echocardiogr 2010;23:240–57;335–7.
14 Flachskampf FA, Badano L, Daniel WG, et al. Recommendations for transoesophageal echocardiography: Update 2010. Eur J Echocardiogr 2010;11:557–76.
15 Picard MH, Adams D, Bierig SM, et al. American Society of Echocardiography recommendations for quality echocardiography laboratory operations. J Am Soc Echocardiogr 2011;24:1–10.
16 Via G, Hussain A, Wells M, et al. International evidence-based recommendations for focused cardiac ultrasound. J Am Soc Echocardiogr 2014;27;683.e681–3.e633.
17 Carerj S, Micari A, Trono A, et al. Anatomical M-mode: An old-new technique. Echocardiography 2003;20:357–61.
18 Henein MY, Gibson DG. Long axis function in disease. Heart 1999;81:229–31.
19 Hu K, Liu D, Herrmann S, et al. Clinical implication of mitral annular plane systolic excursion for patients with cardiovascular disease. Eur Heart J Cardiovasc Imaging 2013;14:205–12.
20 Alam M, Hoglund C, Thorstrand C, et al. Atrioventricular plane displacement in severe congestive heart failure following dilated cardiomyopathy or myocardial infarction. J Intern Med 1990;228:569–75.
21 Hoglund C, Alam M, Thorstrand C. Atrioventricular valve plane displacement in healthy persons. An echocardiographic study. Acta Medica Scandinavica 1998;224:557–62.
22 Willenheimer R, Cline C, Erhardt L, et al. Left ventricular atrioventricular plane displacement: An echocardiographic technique for rapid assessment of prognosis in heart failure. Heart 1997;78:230–6.
23 Matos J, Kronzon I, Panagopoulos G, et al. Mitral annular plane systolic excursion as a surrogate for left ventricular ejection fraction. J Am Soc Echocardiogr 2012;25:969–74.
24 Zidan DH, Helmy TA. Usefulness of mitral annular plane systolic excursion in assessment of left ventricular systolic function in mechanically ventilated obese patients. J Crit Care 2016;34:74–6.
25 Simonson JS, Schiller NB. Descent of the base of the left ventricle: An echocardiographic index of left ventricular function. J Am Soc Echocardiogr 1989;2:25–35.
26 Silva JA, Khuri B, Barbee W, et al. Systolic excursion of the mitral annulus to assess septal function in paradoxic septal motion. Am Heart J 1996;131:138–45.
27 Bergenzaun L, Ohlin H, Gudmundsson P, et al. Mitral annular plane systolic excursion (MAPSE) in shock: A valuable echocardiographic parameter in intensive care patients. Cardiovasc Ultrasound 2013;11:16.
28 Willenheimer R, Israelsson B, Cline C, et al. Left atrioventricular plane displacement is related to both systolic and diastolic left ventricular performance in patients with chronic heart failure. Eur Heart J 1999;20:612–8.
29 Wenzelburger FW, Tan YT, Choudhary FJ, et al. Mitral annular plane systolic excursion on exercise: A simple diagnostic tool for heart failure with preserved ejection fraction. Eur J Heart Fail 2011;13:953–60.
30 El-Battrawy I, Ansari U, Lang S, et al. Risk stratification in Takotsubo syndrome: A role of mitral annular plane systolic excursion. QJM 2018;111:231–6.
31 Huang SJ, Ting I, Huang AM, et al. Longitudinal wall fractional shortening: An M-mode index based on mitral annular plane systolic excursion (MAPSE) that correlates and predicts left ventricular longitudinal strain (LVLS) in intensive care patients. Crit Care 2017;21:292.
32 Terada T, Mori K, Inoue M, et al. Mitral annular plane systolic excursion/left ventricular length (MAPSE/L) as a simple index for assessing left ventricular longitudinal function in children. Echocardiography 2016;33:1703–9.
33 Japp AG, Moir S, Mottram PM. Echocardiographic quantification of left ventricular systolic function. Heart Lung Circ 2015;24:532–5.
34 Emilsson K, Wandt B. The relation between mitral annulus motion and left ventricular ejection fraction in atrial fibrillation. Clin Physiol 2000;20:44–9.
35 Wandt B, Bojo L, Hatle L, et al. Left ventricular contraction pattern changes with age in normal adults. J Am Soc Echocardiogr 1998;11:857–63.
36 Wandt B, Bojo L, Wranne B. Influence of body size and age on mitral ring motion. Clin Physiol 1997;17:635–46.
37 Massie BM, Schiller NB, Ratshin RA, et al. Mitral-septal separation: New echocardiographic index of left ventricular function. Am J Cardiol 1977;39:1008–16.
38 Lew W, Henning H, Schelbert H, et al. Assessment of mitral valve E point-septal separation as an index of left ventricular performance in patients with acute and previous myocardial infarction. Am J Cardiol 1978;41:836–45.
39 Mark DG, Ku BS, Carr BG, et al. Directed bedside transthoracic echocardiography: Preferred cardiac window for left ventricular ejection fraction estimation in critically ill patients. Am J Emerg Med 2007;25:894–900.
40 Ahmadpour H, Shah AA, Allen JW, et al. Mitral E point septal separation: A reliable index of left ventricular performance in coronary artery disease. Am Heart J 1983;106:21–8.
41 Silverstein JR, Laffely NH, Rifkin RD. Quantitative estimation of left ventricular ejection fraction from mitral valve E-point to septal separation and comparison to magnetic resonance imaging. Am J Cardiol 2006;97:137–40.
42 Secko MA, Lazar JM, Salciccioli LA, et al. Can junior emergency physicians use E-point septal separation to accurately estimate left ventricular function in acutely dyspneic patients? Acad Emerg Med 2011;18:1223–6.
43 Child JS, Krivokapich J, Perloff JK. Effect of left ventricular size on mitral E point to ventricular septal separation in assessment of cardiac performance. Am Heart J 1981;101:797–805.
44 McKaigney CJ, Krantz MJ, La Rocque CL, et al. E-point septal separation: A bedside tool for emergency physician assessment of left ventricular ejection fraction. Am J Emerg Med 2014;32:493–7.
45 Lehmann KG, Johnson AD, Goldberger AL. Mitral valve E point-septal separation as an index of left ventricular function with valvular heart disease. Chest 1983;83:102–8.
46 Porter TR, Ornato JP, Guard CS, et al. Transesophageal echocardiography to assess mitral valve function and flow during cardiopulmonary resuscitation. Am J Cardiol 1992;70:1056–60.
47 Toyota S, Amaki Y. Hemodynamic evaluation of the prone position by transesophageal echocardiography. J Clin Anesth 1998;10:32–5.
48 Weekes AJ, Reddy A, Lewis MR, et al. E-point septal separation compared to fractional shortening measurements of systolic function in emergency department patients: Prospective randomized study. J Ultrasound Med 2012;31:1891–7.
49 Lang RM, Bierig M, Devereux RB, et al. Recommendations for chamber quantification. Eur J Echocardiogr 2006;7:79–108.
50 de Simone G, Devereux RB, Roman MJ, et al. Assessment of left ventricular function by the midwall fractional shortening/end-systolic stress relation in human hypertension. J Am Coll Cardiol 1994;23:1444–51.

51 Schussheim AE, Diamond JA, Jhang JS, et al. Midwall fractional shortening is an independent predictor of left ventricular diastolic dysfunction in asymptomatic patients with systemic hypertension. Am J Cardiol 1998;82:1056–9.
52 Weekes AJ, Tassone HM, Babcock A, et al. Comparison of serial qualitative and quantitative assessments of caval index and left ventricular systolic function during early fluid resuscitation of hypotensive emergency department patients. Academic Emerg Med 2011;18:912–21.
53 Jones AE, Craddock PA, Tayal VS, et al. Diagnostic accuracy of left ventricular function for identifying sepsis among emergency department patients with nontraumatic symptomatic undifferentiated hypotension. Shock 2005;24:513–7.
54 Lang RM, Badano LP, Mor-Avi V, et al. Recommendations for chamber quantification. J Am Soc Echocardiogr 2015;28:1–39.
55 Takatsuji H, Mikami T, Urasawa K, et al. A new approach for evaluation of left ventricular diastolic function: Spatial and temporal analysis of left ventricular filling flow propagation by color M-mode Doppler echocardiography. J Am Coll Cardiol 1996;27:365–71.
56 Garcia MJ, Smedira NG, Greenberg NL, et al. Color M-mode Doppler flow propagation velocity is a preload insensitive index of left ventricular relaxation: Animal and human validation. J Am Coll Cardiol 2000;35:201–8.
57 Moller JE, Sondergaard E, Poulsen SH, et al. Pseudonormal and restrictive filling patterns predict left ventricular dilation and cardiac death after a first myocardial infarction: A serial color M-mode Doppler echocardiographic study. J Am Coll Cardiol 2000;36:1841–6.
58 Nagueh SF, Appleton CP, Gillebert TC, et al. Recommendations for the evaluation of left ventricular diastolic function by echocardiography. J Am Soc Echocardiogr 2009;22:107–33.
59 Moller JE, Poulsen SH, Sondergaard E, et al. Preload dependence of color M-mode Doppler flow propagation velocity in controls and in patients with left ventricular dysfunction. J Am Soc Echocardiogr 2000;13:902–9.
60 Steine K, Flogstad T, Stugaard M, et al. Early diastolic intraventricular filling pattern in acute myocardial infarction by color M-mode Doppler echocardiography. J Am Soc Echocardiogr 1998;11:119–25.
61 Garcia MJ, Thomas JD, Klein AL. New Doppler echocardiographic applications for the study of diastolic function. J Am Coll Cardiol 1998;32:865–75.
62 Parthenakis FI, Patrianakos AP, Tzerakis PG, et al. Late left ventricular diastolic flow propagation velocity determined by color M-mode Doppler in the assessment of diastolic dysfunction. J Am Soc Echocardiogr 2004;17:139–45.
63 Patrianakos AP, Parthenakis FI, Mavrakis HE, et al. Late left ventricular color M-mode Doppler in the assessment of diastolic dysfunction in patients with dilated cardiomyopathy. J Am Soc Echocardiogr 2005;18:979.
64 Stewart KC, Kumar R, Charonko JJ, et al. Evaluation of LV diastolic function from color M-mode echocardiography. JACC Cardiovasc Imaging 2011;4:37–46.
65 Garcia MJ, Ares MA, Asher C, et al. An index of early left ventricular filling that combined with pulsed Doppler peak E velocity may estimate capillary wedge pressure. J Am Coll Cardiol 1997;29:448–54.
66 Ueno Y, Nakamura Y, Kinoshita M, et al. Noninvasive estimation of pulmonary capillary wedge pressure by color M-mode Doppler echocardiography in patients with acute myocardial infarction. Echocardiography 2002;19:95–102.
67 Steen T, Steen S. Filling of a model left ventricle studied by colour M mode Doppler. Cardiovasc Res 1994;28:1821–7.
68 Nishihara K, Mikami T, Takatsuji H, et al. Usefulness of early diastolic flow propagation velocity measured by color M-mode Doppler technique for the assessment of left ventricular diastolic function in patients with hypertrophic cardiomyopathy. J Am Soc Echocardiogr 2000;13:801–8.
69 Greyson CR. The right ventricle and pulmonary circulation: Basic concepts. Rev Esp Cardiol 2010;63:81–95.
70 Ho SY, Nihoyannopoulos P. Anatomy, echocardiography, and normal right ventricular dimensions. Heart 2006;92(Suppl 1):i2–13.
71 Argiriou M, Kolokotron SM, Sakellaridis T, et al. Right heart failure post left ventricular assist device implantation. J Thorac Dis 2014;6(Suppl 1):S52–9.
72 Haddad F, Fadel E. RV dysfunction after lung transplantation: A new prognostic marker or mainly a correlate of lung allograft function? JACC Cardiovasc Imaging 2014;7:1095–7.
73 Strumpher J, Jacobsohn E. Pulmonary hypertension and right ventricular dysfunction: Physiology and perioperative management. J Cardiothorac Vasc Anesth 2011;25:687–704.
74 Aloia E, Cameli M, D'Ascenzi F, et al. TAPSE: An old but useful tool in different diseases. Int J Cardiol 2016;225:177–83.
75 Rudski LG, Lai WW, Afilalo J, et al. Guidelines for the echocardiographic assessment of the right heart in adults: A report from the American Society of Echocardiography endorsed by the European Association of Echocardiography, a registered branch of the European Society of Cardiology, and the Canadian Society of Echocardiography. J Am Soc Echocardiogr 2010;23:685–713;quiz 786–8.
76 Miller D, Farah MG, Liner A, et al. The relation between quantitative right ventricular ejection fraction and indices of tricuspid annular motion and myocardial performance. J Am Soc Echocardiogr 2004;17:443–7.
77 Lopez-Candales A, Dohi K, Rajagopalan N, et al. Defining normal variables of right ventricular size and function in pulmonary hypertension: An echocardiographic study. Postgraduate Med J 2008;84:40–5.
78 Kaul S, Tei C, Hopkins JM, et al. Assessment of right ventricular function using two-dimensional echocardiography. Am Heart J 1984;107:526–31.
79 Kopecna D, Briongos S, Castillo H, et al. Interobserver reliability of echocardiography for prognostication of normotensive patients with pulmonary embolism. Cardiovasc Ultrasound 2014;12:29.
80 Korshin A, Gronlykke L, Nilsson JC, et al. The feasibility of tricuspid annular plane systolic excursion performed by transesophageal echocardiography throughout heart surgery and its interchangeability with transthoracic echocardiography. Int J Cardiovasc Imaging 2018;34:1017–28.
81 Akiyama K, Arisawa S, Ide M, et al. Intraoperative cardiac assessment with transesophageal echocardiography for decision-making in cardiac anesthesia. Gen Thorac Cardiovascular Surg 2013;61:320–9.
82 Forfia PR, Fisher MR, Mathai SC, et al. Tricuspid annular displacement predicts survival in pulmonary hypertension. Am J Respiratory Crit Care Med 2006;174:1034–41.
83 Sato T, Tsujino I, Oyama-Manabe N, et al. Simple prediction of right ventricular ejection fraction using tricuspid annular plane systolic excursion in pulmonary hypertension. International J Cardiovascular Imaging 2013;29:1799–805.
84 Harrison A, Hatton N, Ryan JJ. The right ventricle under pressure: Evaluating the adaptive and maladaptive changes in the right ventricle in pulmonary arterial hypertension using echocardiography (2013 Grover Conference series). Pulm Circ 2015;5:29–47.
85 Daley J, Grotberg J, Pare J, et al. Emergency physician performed tricuspid annular plane systolic excursion in the evaluation of suspected pulmonary embolism. Am J Emerg Med 2017;35:106–11.
86 Rydman R, Soderberg M, Larsen F, et al. Echocardiographic evaluation of right ventricular function in patients with acute pulmonary embolism: A study using tricuspid annular motion. Echocardiography 2010;27:286–93.
87 Fichet J, Moreau L, Genee O, et al. Feasibility of right ventricular longitudinal systolic function evaluation with transthoracic echocardiographic indices derived from tricuspid annular motion: A preliminary study in acute respiratory distress syndrome. Echocardiography 2012;29:513–21.
88 Damy T, Kallvikbacka-Bennett A, Goode K, et al. Prevalence of, associations with, and prognostic value of tricuspid annular plane systolic excursion (TAPSE) among out-patients referred for the evaluation of heart failure. J Cardiac Fail 2012;18:216–25.
89 Ereminiene E, Vaskelyte JJ, Stoskute N, et al. Determinants of reduced tricuspid annular plane systolic excursion in patients with severe systolic left ventricular dysfunction. Acta Cardiologica 2012;67:657–63.
90 Ghio S, Recusani F, Klersy C, et al. Prognostic usefulness of the tricuspid annular plane systolic excursion in patients with congestive heart failure secondary to idiopathic or ischemic dilated cardiomyopathy. Am J Cardiol 2000;85:837–42.
91 Okada DR, Rahmouni HW, Herrmann HC, et al. Assessment of right ventricular function by transthoracic echocardiography following aortic valve replacement. Echocardiography 2014;31:552–7.

92 Gajanana D, Seetha Rammohan H, Alli O, et al. Tricuspid annular plane systolic excursion and its association with mortality in critically ill patients. Echocardiography 2015;32:1222–7.
93 Lamia B, Teboul JL, Monnet X, et al. Relationship between the tricuspid annular plane systolic excursion and right and left ventricular function in critically ill patients. Intensive Care Med 2007;33:2143–9.
94 Vonk Noordegraaf A, Westerhof BE, Westerhof N. The relationship between the right ventricle and its load in pulmonary hypertension. J Am Coll Cardiol 2017;69:236–43.
95 Diaz-Gomez JL, Alvarez AB, Danaraj JJ, et al. A novel semiquantitative assessment of right ventricular systolic function with a modified subcostal echocardiographic view. Echocardiography 2017;34:44–52.
96 de Agustin JA, Martinez-Losas P, de Diego JJ, et al. Tricuspid annular plane systolic excursion inaccuracy to assess right ventricular function in patients with previous tricuspid annulopasty. Int J Cardiol 2016;223:713–6.
97 Lindqvist P, Henein M, Kazzam E. Right ventricular outflow-tract fractional shortening: An applicable measure of right ventricular systolic function. Eur J Echocardiogr 2003;4:29–35.
98 Allam LE, Onsy AM, Ghalib HA. Right ventricular outflow tract systolic excursion and fractional shortening: Can these echocardiographic parameters be used for the assessment of right ventricular function? J Cardiovasc Echogr 2017;27:52–8.
99 Yamaguchi M, Tsuruda T, Watanabe Y, et al. Reduced fractional shortening of right ventricular outflow tract is associated with adverse outcomes in patients with left ventricular dysfunction. Cardiovasc Ultrasound 2013;11:19.
100 Sahan E, Karamanlioglu M, Sahan S, et al. The relationship between right ventricular outflow tract fractional shortening and Pulmonary Embolism Severity Index in acute pulmonary embolism. Turk Kardiyoloji Dernegi Ars 2017;45:709–14.
101 Unluer EE, Yavasi O, Akoglu H, et al. Bedside assessment of central venous pressure by sonographic measurement of right ventricular outflow-tract fractional shortening. Eur J Emerg Med 2013;20:18–22.
102 Ryan T, Petrovic O, Dillon JC, et al. An echocardiographic index for separation of right ventricular volume and pressure overload. J Am Coll Cardiol 1985;5:918–27.
103 Jardin F, Dubourg O, Gueret P, et al. Quantitative two-dimensional echocardiography in massive pulmonary embolism: Emphasis on ventricular interdependence and leftward septal displacement. J Am Coll Cardiol 1987;10:1201–6.
104 Kumar A, Falke KJ, Geffin B, et al. Continuous positive-pressure ventilation in acute respiratory failure. N Engl J Med 1970;283:1430–6.
105 Jardin F, Farcot JC, Boisante L, et al. Influence of positive end-expiratory pressure on left ventricular performance. N Engl J Med 1981;304:387–92.
106 Jardin F, Farcot JC, Boisante L, et al. Mechanism of paradoxic pulse in bronchial asthma. Circulation 1982;66:887–94.
107 Mori S, Nakatani S, Kanzaki H, et al. Patterns of the interventricular septal motion can predict conditions of patients with pulmonary hypertension. J Am Soc Echocardiogr 2008;21:386–93.
108 Abbasi AS, Eber LM, MacAlpin RN, et al. Paradoxical motion of interventricular septum in left bundle branch block. Circulation 1974;49:423–7.
109 Kerber RE, Litchfield R. Postoperative abnormalities of interventricular septal motion: Two-dimensional and M-mode echocardiographic correlations. Am Heart J 1982;104:263–8.
110 Vignola PA, Boucher CA, Curfman GD, et al. Abnormal interventricular septal motion following cardiac surgery: Clinical, surgical, echocardiographic and radionuclide correlates. Am Heart J 1979;97:27–34.
111 Tsuda T, Sawayama T, Kawai N, et al. Echocardiographic measurement of right ventricular wall thickness in adults by anterior approach. Br Heart J 1980;44:55–61.
112 Gottdiener JS, Gay JA, Maron BJ, et al. Increased right ventricular wall thickness in left ventricular pressure overload: Echocardiographic determination of hypertrophic response of the "nonstressed" ventricle. J Am Coll Cardiol 1985;6:550–5.
113 Vieillard-Baron A, Prin S, Chergui K, et al. Echo-Doppler demonstration of acute cor pulmonale at the bedside in the medical intensive care unit. Am J Respiratory Crit Care Med 2002;166:1310–9.
114 Yamamoto S, Sawayama T, Nezuo S, et al. [Usefulness of measuring right ventricular anterior wall thickness in patients with right ventricular overload using M-mode echocardiography]. J Cardiol 1987;17:837–43.
115 Simon MA, Deible C, Mathier MA, et al. Phenotyping the right ventricle in patients with pulmonary hypertension. Clin Translational Sci 2009;2:294–9.
116 McKenna WJ, Kleinebenne A, Nihoyannopoulos P, et al. Echocardiographic measurement of right ventricular wall thickness in hypertrophic cardiomyopathy: Relation to clinical and prognostic features. J Am Coll Cardiol 1988;11:351–8.
117 Denault AY, Chaput M, Couture P, et al. Dynamic right ventricular outflow tract obstruction in cardiac surgery. J Thorac Cardiovasc Surg 2006;132:43–9.
118 Gorcsan J 3rd, Reddy SC, Armitage JM, et al. Acquired right ventricular outflow tract obstruction after lung transplantation: Diagnosis by transesophageal echocardiography. J Am Soc Echocardiogr 1993;6:324–6.
119 Malik R, Maron MS, Rastegar H, et al. Hypertrophic cardiomyopathy with right ventricular outflow tract and left ventricular intracavitary obstruction. Echocardiography 2014;31:682–5.
120 Karmarkar S. Pulmonary valve echocardiography. J Postgraduate Med 1979;25:219–23.
121 Kirshbom PM, Tapson VF, Harrison JK, et al. Delayed right heart failure following lung transplantation. Chest 1996;109:575–7.
122 Barbier C, Loubieres Y, Schmit C, et al. Respiratory changes in inferior vena cava diameter are helpful in predicting fluid responsiveness in ventilated septic patients. Intensive Care Med 2004;30:1740–6.
123 Brennan JM, Ronan A, Goonewardena S, et al. Handcarried ultrasound measurement of the inferior vena cava for assessment of intravascular volume status in the outpatient hemodialysis clinic. Clin J Am Soc Nephrol 2006;1:749–53.
124 Ciozda W, Kedan I, Kehl DW, et al. The efficacy of sonographic measurement of inferior vena cava diameter as an estimate of central venous pressure. Cardiovasc Ultrasound 2016;14:33.
125 Brennan JM, Blair JE, Goonewardena S, et al. Reappraisal of the use of inferior vena cava for estimating right atrial pressure. J Am Soc Echocardiogr 2007;20:857–61.
126 Porter TR, Shillcutt SK, Adams MS, et al. Guidelines for the use of echocardiography as a monitor for therapeutic intervention in adults: A report from the American Society of Echocardiography. J Am Soc Echocardiogr 2015;28:40–56.
127 Lanspa MJ, Grissom CK, Hirshberg EL, et al. Applying dynamic parameters to predict hemodynamic response to volume expansion in spontaneously breathing patients with septic shock. Shock 2013;39:155–60.
128 Thanakitcharu P, Charoenwut M, Siriwiwatanakul N. Inferior vena cava diameter and collapsibility index: A practical non-invasive evaluation of intravascular fluid volume in critically-ill patients. J Med Assoc Thailand 2013;96(Suppl 3):S14–22.
129 Airapetian N, Maizel J, Alyamani O, et al. Does inferior vena cava respiratory variability predict fluid responsiveness in spontaneously breathing patients? Crit Care 2015;19:400.
130 Muller L, Bobbia X, Toumi M, et al. Respiratory variations of inferior vena cava diameter to predict fluid responsiveness in spontaneously breathing patients with acute circulatory failure: Need for a cautious use. Crit Care 2012;16:R188.
131 Preau S, Bortolotti P, Colling D, et al. Diagnostic accuracy of the inferior vena cava collapsibility to predict fluid responsiveness in spontaneously breathing patients with sepsis and acute circulatory failure. Crit Care Med 2017;45:e290–7.
132 Schmidt GA, Koenig S, Mayo PH. Shock: Ultrasound to guide diagnosis and therapy. Chest 2012;142:1042–8.
133 Walley PE, Walley KR, Goodgame B, et al. A practical approach to goal-directed echocardiography in the critical care setting. Crit Care 2014;18:681.
134 Perera P, Mailhot T, Riley D, et al. The RUSH exam: Rapid Ultrasound in SHock in the evaluation of the critically ill. Emerg Med Clin N Am 2010;28:29–56;vii.
135 Ceruti S, Anselmi L, Minotti B, et al. Prevention of arterial hypotension after spinal anaesthesia using vena cava ultrasound to guide fluid management. Br J Anaesth 2018;120:101–8.

136 Blehar DJ, Resop D, Chin B, et al. Inferior vena cava displacement during respirophasic ultrasound imaging. Crit Ultrasound J 2012;4:18.
137 Gignon L, Roger C, Bastide S, et al. Influence of diaphragmatic motion on inferior vena cava diameter respiratory variations in healthy volunteers. Anesthesiology 2016;124:1338–46.
138 Wallace DJ, Allison M, Stone MB. Inferior vena cava percentage collapse during respiration is affected by the sampling location: An ultrasound study in healthy volunteers. Academ Emerg Med 2010;17:96–9.
139 Goldhammer E, Mesnick N, Abinader EG, et al. Dilated inferior vena cava: A common echocardiographic finding in highly trained elite athletes. J Am Soc Echocardiogr 1999;12:988–93.
140 Arthur ME, Landolfo C, Wade M, et al. Inferior vena cava diameter (IVCD) measured with transesophageal echocardiography (TEE) can be used to derive the central venous pressure (CVP) in anesthetized mechanically ventilated patients. Echocardiography 2009;26:140–9.
141 Feissel M, Michard F, Faller JP, et al. The respiratory variation in inferior vena cava diameter as a guide to fluid therapy. Intensive Care Med 2004;30:1834–7.
142 Moretti R, Pizzi B. Inferior vena cava distensibility as a predictor of fluid responsiveness in patients with subarachnoid hemorrhage. Neurocrit Care 2010;13:3–9.
143 Vignon P, Repesse X, Begot E, et al. Comparison of echocardiographic indices used to predict fluid responsiveness in ventilated patients. Am J Respiratory Crit Care Med 2017;195:1022–32.
144 Bentzer P, Griesdale DE, Boyd J, et al. Will this hemodynamically unstable patient respond to a bolus of intravenous fluids? JAMA 2016;316:1298–309.
145 Vieillard-Baron A, Evrard B, Repesse X, et al. Limited value of end-expiratory inferior vena cava diameter to predict fluid responsiveness impact of intra-abdominal pressure. Intensive Care Med 2018;44:197–203.
146 Juhl-Olsen P, Frederiksen CA, Sloth E. Ultrasound assessment of inferior vena cava collapsibility is not a valid measure of preload changes during triggered positive pressure ventilation: A controlled cross-over study. Ultraschall Med 2012;33:152–9.
147 Vieillard-Baron A, Augarde R, Prin S, et al. Influence of superior vena caval zone condition on cyclic changes in right ventricular outflow during respiratory support. Anesthesiology 2001;95:1083–8.
148 Vieillard-Baron A, Chergui K, Rabiller A, et al. Superior vena caval collapsibility as a gauge of volume status in ventilated septic patients. Intensive Care Med 2004;30:1734–9.
149 Cowie BS, Kluger R, Rex S, et al. The relationship between superior vena cava diameter and collapsibility and central venous pressure. Anaesth Intensive Care 2015;43:357–60.
150 Azarbal A, LeWinter MM. Pericardial effusion. Cardiol Clin 2017;35:515–24.
151 Armstrong WF, Schilt BF, Helper DJ, et al. Diastolic collapse of the right ventricle with cardiac tamponade: An echocardiographic study. Circulation 1982;65:1491–6.
152 Klein AL, Abbara S, Agler DA, et al. American Society of Echocardiography clinical recommendations for multimodality cardiovascular imaging of patients with pericardial disease: Endorsed by the Society for Cardiovascular Magnetic Resonance and Society of Cardiovascular Computed Tomography. J Am Soc Echocardiogr 2013;26:965–1012;e1015.
153 Niarchos AP. Electrical alternans in cardiac tamponade. Thorax 1975;30:228–33.
154 Vignola PA, Pohost GM, Curfman GD, et al. Correlation of echocardiographic and clinical findings in patients with pericardial effusion. Am J Cardiol 1976;37:701–7.
155 Appleton C, Gillam L, Koulogiannis K. Cardiac tamponade. Cardiol Clin 2017;35:525–37.
156 Varghese R, Itagaki S, Anyanwu AC, et al. Predicting systolic anterior motion after mitral valve reconstruction: Using intraoperative transoesophageal echocardiography to identify those at greatest risk. Eur J Cardiothorac Surg 2014;45:132–7;discussion 137–8.
157 Nakamura T, Sekiya N, Nakazato T, et al. Systolic anterior motion of the mitral valve masked by general anesthesia. Asian Cardiovasc Thorac Ann 2014;22:197–9.
158 Chauvet JL, El-Dash S, Delastre O, et al. Early dynamic left intraventricular obstruction is associated with hypovolemia and high mortality in septic shock patients. Crit Care 2015;19:262.
159 Auer J, Berent R, Weber T, et al. Catecholamine therapy inducing dynamic left ventricular outflow tract obstruction. Int J Cardiol 2005;101:325–8.
160 Izgi C, Akgun T, Men EE, et al. Systolic anterior motion of the mitral valve in the absence left ventricular hypertrophy: Role of mitral leaflet elongation and papillary muscle displacement. Echocardiography 2010;27:E36–8.
161 Luckie M, Khattar RS. Systolic anterior motion of the mitral valve–beyond hypertrophic cardiomyopathy. Heart 2008;94:1383–5.
162 Yang JH, Park SW, Yang JH, et al. Dynamic left ventricular outflow tract obstruction without basal septal hypertrophy, caused by catecholamine therapy and volume depletion. Korean J Intern Med 2008;23:106–9.
163 Pollick C, Rakowski H, Wigle ED. Muscular subaortic stenosis: The quantitative relationship between systolic anterior motion and the pressure gradient. Circulation 1984;69:43–9.
164 Choudhury L, Rigolin VH, Bonow RO. Integrated imaging in hypertrophic cardiomyopathy. Am J Cardiol 2017;119:328–39.
165 Popescu BA, Rosca M, Schwammenthal E. Dynamic obstruction in hypertrophic cardiomyopathy. Curr Opin Cardiol 2015;30:468–74.
166 Luckner G, Margreiter J, Jochberger S, et al. Systolic anterior motion of the mitral valve with left ventricular outflow tract obstruction: Three cases of acute perioperative hypotension in noncardiac surgery. Anesth Analg 2005;100:1594–8.
167 Nagueh SF, Bierig SM, Budoff MJ, et al. American Society of Echocardiography clinical recommendations for multimodality cardiovascular imaging of patients with hypertrophic cardiomyopathy: Endorsed by the American Society of Nuclear Cardiology, Society for Cardiovascular Magnetic Resonance, and Society of Cardiovascular Computed Tomography. J Am Soc Echocardiogr 2011;24:473–98.
168 Labovitz AJ, Noble VE, Bierig M, et al. Focused cardiac ultrasound in the emergent setting: A consensus statement of the American Society of Echocardiography and American College of Emergency Physicians. J Am Soc Echocardiogr 2010;23:1225–30.
169 Hahn RT, Abraham T, Adams MS, et al. Guidelines for performing a comprehensive transesophageal echocardiographic examination: Recommendations from the American Society of Echocardiography and the Society of Cardiovascular Anesthesiologists. J Am Soc Echocardiogr 2013;26:921–64.
170 Nanda NC, Gramiak R, Shah PM. Diagnosis of aortic root dissection by echocardiography. Circulation 1973;48:506–13.
171 Evangelista A, Garcia-del-Castillo H, Gonzalez-Alujas T, et al. Diagnosis of ascending aortic dissection by transesophageal echocardiography: Utility of M-mode in recognizing artifacts. J Am Coll Cardiol 1996;27:102–7.
172 D'Cruz IA, Jain M, Campbell C, et al. Ultrasound visualization of aortic dissection by right parasternal scanning, including systolic flutter of the intimal flap. Chest 1981;80:239–42.
173 Sheka K, Sadiq A, Kabalkin C, et al. The use of M-mode echocardiography to identify the true lumen in aortic dissection. J Am Soc Echocardiogr 2004;17:1309–10.
174 Mahmood F, Shernan SK. Perioperative transoesophageal echocardiography: Current status and future directions. Heart 2016;102:1159–67.
175 Muralidhar K. Utility of perioperative transesophageal echocardiography. Ann Cardiac Anaesth 2016;19:S2–5.
176 Nienaber CA, von Kodolitsch Y, Nicolas V, et al. The diagnosis of thoracic aortic dissection by noninvasive imaging procedures. N Engl J Med 1993;328:1–9.
177 Penco M, Paparoni S, Dagianti A, et al. Usefulness of transesophageal echocardiography in the assessment of aortic dissection. Am J Cardiol 2000;86:53G–6.
178 D'Cruz IA, Jain DP, Hirsch L, et al. Echocardiographic diagnosis of dilatation of the ascending aorta using right parasternal scanning. Radiology 1978;129:465–9.
179 Roudaut RP, Billes MA, Gosse P, et al. Accuracy of M-mode and two-dimensional echocardiography in the diagnosis of aortic dissection: An experience with 128 cases. Clin Cardiol 1988;11:553–62.
180 Alter P, Herzum M, Maisch B. Echocardiographic findings mimicking type A aortic dissection. Herz 2006;31:153–5.